USGS
science for a changing world

Processes of Terrace Formation on the Piedmont of the Santa Cruz River Valley During Quaternary Time, Green Valley-Tubac Area, Southeastern Arizona

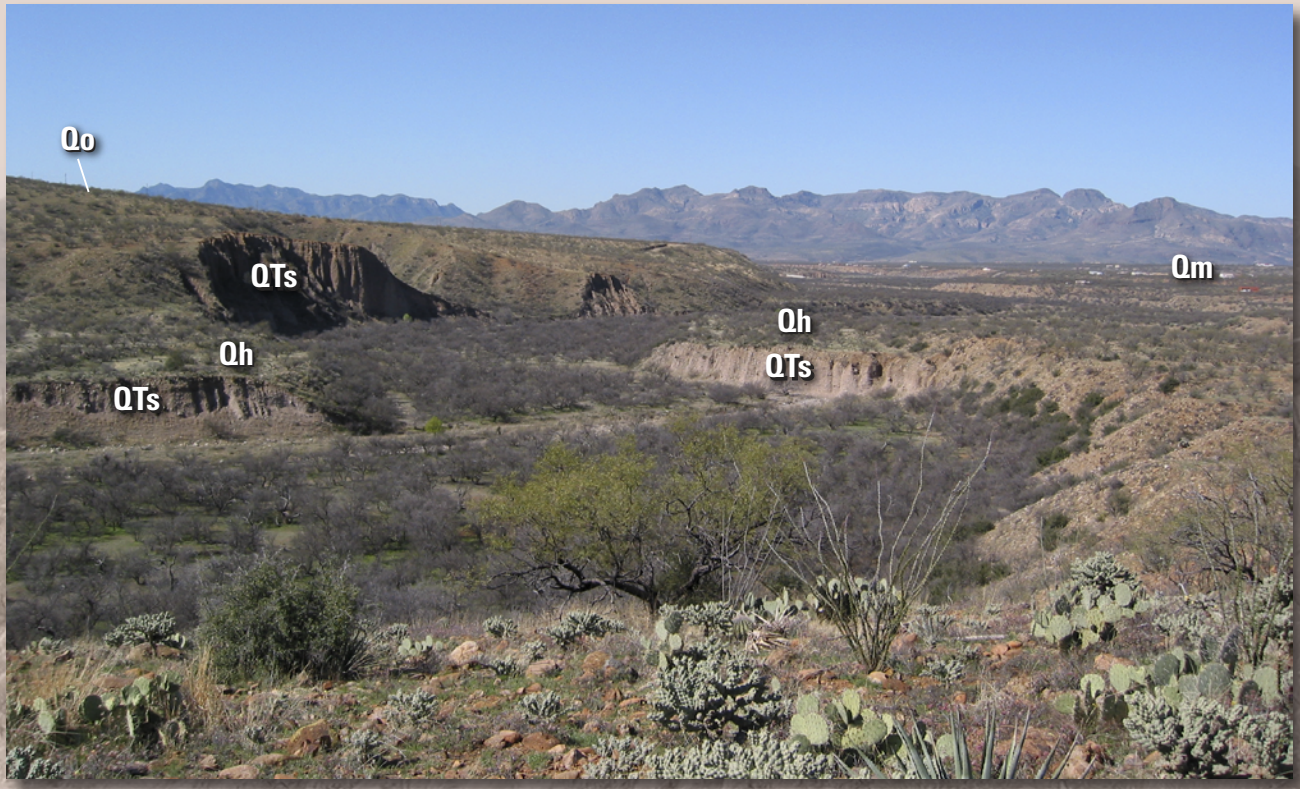

Scientific Investigations Report 2010–5028

U.S. Department of the Interior
U.S. Geological Survey

Cover. Stepped terraces of Josephine Canyon Wash, looking downstream (west). Qh, Holocene terrace; Qm, middle Pleistocene terrace; Qo, early Pleistocene terrace; QTs, early Pleistocene to Pliocene alluvium. Early Pleistocene terraces on south (left) side of stream are graded to San Cayetano Mountains.

Processes of Terrace Formation on the Piedmont of the Santa Cruz River Valley During Quaternary Time, Green Valley-Tubac Area, Southeastern Arizona

By David A. Lindsey and Bradley S. Van Gosen

A description of terrace gravel on the piedmont of southeastern Arizona and what it reveals about the origin of terraces

Scientific Investigations Report 2010–5028

U.S. Department of the Interior
U.S. Geological Survey

U.S. Department of the Interior
KEN SALAZAR, Secretary

U.S. Geological Survey
Marcia K. McNutt, Director

U.S. Geological Survey, Reston, Virginia: 2010

For more information on the USGS—the Federal source for science about the Earth, its natural and living resources, natural hazards, and the environment, visit http://www.usgs.gov or call 1-888-ASK-USGS

For an overview of USGS information products, including maps, imagery, and publications, visit http://www.usgs.gov/pubprod

To order this and other USGS information products, visit http://store.usgs.gov

Any use of trade, product, or firm names is for descriptive purposes only and does not imply endorsement by the U.S. Government.

Although this report is in the public domain, permission must be secured from the individual copyright owners to reproduce any copyrighted materials contained within this report.

Suggested citation:
Lindsey, D.A., and Van Gosen, B.S., 2010, Processes of terrace formation on the Piedmont of the Santa Cruz River valley during Quaternary time, Green Valley-Tubac area, southeastern Arizona: U.S. Geological Survey Scientific Investigations Report 2010–5028, 39 p.

Contents

Abstract 1
Introduction 1
Alluvial History 2
Terrace Classification and Formation 6
Terrace Deposits 9
Gravel Lithology 15
Particle Size and Sorting 18
Discussion and Conclusions 24
References Cited 25
Appendix A. Pebble Lithology and Roundness Counts 28
Appendix B. Particle Size Data 36

Figures

1–2. Maps showing:
1. Generalized geology of upper Tertiary and Quaternary alluvium of the Santa Cruz River valley, Green Valley-Tubac area, Arizona 3
2. Details of upper Tertiary and Quaternary alluvium in the upper part of Josephine Canyon 5

3–6. Photographs of:
3. Formation of erosional terraces on Josephine Canyon Wash 7
4. Erosional terraces 10
5. Middle Pleistocene depositional terrace on Josephine Canyon Wash 12
6. Sedimentary features in depositional terraces near the mountain front 13

7–8. Pie diagrams showing:
7. Summaries of clast lithology for early Pleistocene to Holocene gravel 16
8. Summaries of clast lithology for gravel of Madera Canyon Wash as it changed course during Pleistocene time 17

9–11. Cumulative frequency curves for:
9. Cumulative frequency curves for particle size in gravel of varying age and distance from the canyon mouth of Montosa Canyon Wash. A, Upper piedmont; B, Lower piedmont 19
10. Cumulative frequency curves for particle size in gravel deposited by Madera Canyon Wash and Florida Canyon Wash 20
11. Cumulative frequency curves for particle size in gravel of varying age within a 3-km reach of Josephine Canyon Wash 22

12. Graphs showing thickness, sorting, and particle-size relations for terrace fill 22

Table

1. Comparison of mountain bedrock catchment basins....6

Appendix Tables

A1. Sample locations for pebble counts of terrace gravel....29
A2. Summary of pebble counts for terrace gravel....30
A3. Lithology versus roundness for terrace gravel of Madera Canyon Wash and adjacent streams....31
A4. Lithology versus roundness for terrace gravel of Montosa Canyon Wash....32
A5. Lithology versus roundness for terrace gravel of Cottonwood Canyon Wash....33
A6. Lithology versus roundness for terrace gravel of Josephine Canyon Wash....34
A7. Chi-square analysis of pebble lithology versus roundness....35
B1. Volumetric particle size data and statistics for terrace gravel....37
B2. Classification of particle size samples by local area and stratigraphic unit....39

Processes of Terrace Formation on the Piedmont of the Santa Cruz River Valley During Quaternary Time, Green Valley-Tubac Area, Southeastern Arizona

By David A. Lindsey and Bradley S. Van Gosen

Abstract

In this report we describe a series of stepped Quaternary terraces on some piedmont tributaries of the Santa Cruz River valley in southeastern Arizona. These terraces began to form in early Pleistocene time, after major basin-and-range faulting ceased, with lateral planation of basin fill and deposition of thin fans of alluvium. At the end of this cycle of erosion and deposition, tributaries of the Santa Cruz River began the process of dissection and terrace formation that continues to the present. Vertical cutting alternated with periods of equilibrium, during which streams cut laterally and left thin deposits of channel fill.

The distribution of terraces was mapped and compiled with adjacent mapping to produce a regional picture of piedmont stream history in the middle part of the Santa Cruz River valley. For selected tributaries, the thickness of terrace fill was measured, particle size and lithology of gravel were determined, and sedimentary features were photographed and described. Mapping of terrace stratigraphy revealed that on two tributaries, Madera Canyon Wash and Montosa Canyon Wash, stream piracy has played an important role in piedmont landscape development. On two other tributaries, Cottonwood Canyon Wash and Josephine Canyon Wash, rapid downcutting preempted piracy.

Two types of terraces are recognized: erosional and depositional. Gravel in thin erosional terraces has Trask sorting coefficients and sedimentary structures typical of streamflood deposits, replete with bar-and-swale surface topography on young terraces. Erosional-terrace fill represents the channel fill of the stream that cuts the terrace; the thickness of the fill indicates the depth of channel scour. In contrast to erosional terraces, depositional terraces show evidence of repeated deposition and net aggradation, as indicated by their thickness (as much as 20+ m) and weakly bedded structure. Depositional terraces are common below mountain-front canyon mouths where streams drop their load in response to abrupt flattening of gradients and expansion of channel banks, and they extend down the piedmont along Josephine Canyon Wash. Gravel in depositional terraces also has sorting coefficients typical of streamflood deposits. Sedimentary features in both types of terraces are consistent with deposition by flash floods in ephemeral streams, suggesting the climate was arid. Bedding and clast armor are weakly developed, clast clusters and imbrication are common, and crossbedding is generally absent. Debris-flow deposits, even near the mountain front, are surprisingly rare.

On the tectonically stable piedmont of southeastern Arizona, stream piracy and climate change are the most likely agents of terrace formation. Both piracy and climate change can cause rapid changes in discharge and sediment supply, which initiate cycles of incision, lateral cutting, and aggradation. Increased stream discharge initiates downcutting, but increased sediment supply interrupts downcutting and causes streams to cut laterally and aggrade. At times, on Madera Canyon Wash and Montosa Canyon Wash, stream piracy affected stream discharge and sediment supply, but on Cottonwood Canyon Wash and Josephine Canyon Wash, only climate change could have initiated terrace cutting. Terraces probably formed during extended arid intervals when sparse vegetation and flashy stream discharge combined to increase sediment supply. In most cases, sediment supply was sufficient to promote lateral cutting but not long-term aggradation. Thus, most streams formed erosional terraces. The middle Pleistocene Josephine Canyon Wash formed a depositional terrace because it had a source of abundant unconsolidated sediment.

Introduction

Since the end of basin-and-range faulting and basin filling in Pliocene time (Menges and McFadden, 1981), streams emerging from the mountains have cut landscapes of canyons and stepped terraces in the piedmont of southeastern Arizona. Periods of downcutting (canyon incision) alternated with lateral cutting (terrace formation) and, occasionally, deposition of terrace fill, but the mechanisms for this alternation are obscure. Climate change and tectonism both cause terraces to form (Bull, 1991; Leopold and others, 1964), but we know only the general outlines of Quaternary climate history and tectonism of the region. The relative age of some terraces has been determined by studies of weathering and soil

development (for example, Helmick, 1986), and more recently the distribution and relative age of piedmont terraces in many areas have been mapped by staff of the Arizona Geological Survey. Sedimentologic descriptions of terrace deposits were lacking, so depositional processes were not well known.

Here we bring together results of geologic mapping and sedimentologic study of piedmont terraces in southeastern Arizona to interpret the processes that formed these terraces. We use the distribution and morphology of terraces and the lithology of terrace gravel to identify cases of stream piracy, and we use the sedimentologic features of terrace gravel to interpret depositional processes. Much of the data on terrace geomorphology was gathered while mapping part of the Mount Hopkins and San Cayetano Mountains 7.5′ quadrangles (Lindsey and Van Gosen, 2006). This map and maps of surrounding quadrangles made by staff of the Arizona Geological Survey (Pearthree and Youberg, 2000; Spencer and others, 2003; and Youberg and Helmick, 2001), show the distribution of terraces formed during Pleistocene and Holocene time (fig. 1).

On the arid piedmont of southeastern Arizona, sand and gravel are deposited during brief, intense storms that trigger floods and landslides (Field, 1994; Klawon and Pearthree, 2000; Pearthree and Youberg, 2006). In ephemeral streams, a variety of fluid flows, ranging from debris flow to channel flow to sheet wash, can leave behind sand and gravel deposits ranging from poorly sorted and unstratified to well-sorted and stratified (Blair and McPherson, 1994; Costa, 1988; Lindsey and Melick, 2002). Cooler, wetter conditions than today may have prevailed in southeastern Arizona during late Pleistocene time (Davis, 1999; Thompson and others, 2003), allowing some piedmont streams to flow continuously. Deposits of perennial streams differ from those of ephemeral streams. In perennial streams, like those of the semiarid Colorado piedmont, storm-generated streamfloods deposit well-stratified and cross-stratified sand and gravel in channel and bank-attached bars (Lindsey and others, 2005). In this report, sedimentary features (fill thickness, particle size, sorting, and sedimentary structures) are used to assess continuity of streamflow and alluvial depositional processes on the Arizona piedmont.

Alluvial History

The alluvial history of the Santa Cruz River valley, like that of most other basins in southern Arizona and New Mexico, can be divided into two phases: (1) Miocene and Pliocene basin filling and (2) late Pliocene to Holocene erosion (Connell and others, 2005; Menges and McFadden, 1981; Menges and Pearthree, 1989). During phase 1, basin-and-range faulting formed a string of basins in the upper Santa Cruz River valley that defined the future course of the river (Gettings and Houser, 1997). Piedmont alluvial fans deposited poorly sorted sand and gravel of the Miocene and Pliocene Nogales Formation (Simons, 1974) and other units assigned to the lower part of the basin fill (Gettings and Houser, 1997). Basin-and-range faulting in southeastern Arizona had largely ended by Pliocene time, as indicated by the relatively undeformed upper part of the basin fill (Menges and Pearthree, 1989). The Santa Cruz River basin was probably closed downstream near Tucson, Ariz., as indicated by playa deposits in the subsurface (Houser and others, 2004). Phase 2 most likely began with integration of the Santa Cruz River basin into the Gila River drainage in late Pliocene or early Pleistocene time (Connell and others, 2005; Menges and Pearthree, 1989). Tributary streams of the Santa Cruz River began to dissect basin fill and cut pediments capped by coarse gravel. Phase 2 was accompanied by only minor faulting where, for example, faults displace early and middle Pleistocene age terrace deposits near Cottonwood Canyon Wash (Lindsey and Van Gosen, 2006) and terraces of early to late Pleistocene age north of Madera Canyon Wash (Pearthree and Youberg, 2000).

Pleistocene and Holocene alluvial deposits in the valley of the Santa Cruz River (Youberg and Helmick, 2001) consist of (1) river alluvium, deposited by the Santa Cruz River, and (2) piedmont alluvium, deposited by tributary streams draining the adjacent mountain ranges (fig. 1). As the master stream, the Santa Cruz River defines base level for its tributary streams. The extent of piedmont deposits in the Santa Cruz River valley has been influenced by rates of deposition and by local structural features. In response to uplift of the Santa Rita Mountains and extensive development of alluvial fans on the eastern side of the Santa Cruz River valley during phase 1, the river flows nearer the west side than the east side of the valley (fig. 1). South of Madera Canyon Wash, the valley is confined to a narrow faulted basin between the Tumacacori and Santa Rita Mountains (Gettings and Houser, 1997).

In the Santa Cruz River valley, the oldest records of phase 2 piedmont erosion are early Pleistocene pediments capped by thin gravel deposits. In the study area, the gravels seldom exceed 20 m in thickness and rest on older basin fill and bedrock. In map view (figs. 1 and 2), these deposits form distinctive bird-foot outlines that extend out from the mouths of mountain canyons. They are interpreted as dissected alluvial fans; the bird-foot pattern represents inverted radiating channels. The channels are preserved as inverted topography because they are filled with coarse gravel that resisted erosion (Ritter, 1987). For comparison, on the Colorado piedmont north of Denver, Colo., the Rocky Flats fan provides a good example of the early stages of dissection; the inverted channels in this fan have been documented by numerous boreholes (Knepper, 2005; Lindsey and others, 2005). On the Arizona piedmont east of Green Valley and Tubac, Ariz., the distinctive bird-foot map pattern is evident at the mouths of Madera Canyon, Montosa Canyon, and Josephine Canyon. Other thin dissected fans have been described from southeastern Arizona as “red-soil fans” (Melton, 1965), after their characteristic soil color, and “pediment fans” (Menges and McFadden, 1981), after their occurrence on erosional surfaces cut on bedrock. All of these fans are thinner and perhaps coarser grained and better sorted than alluvial fans deposited in tectonically active

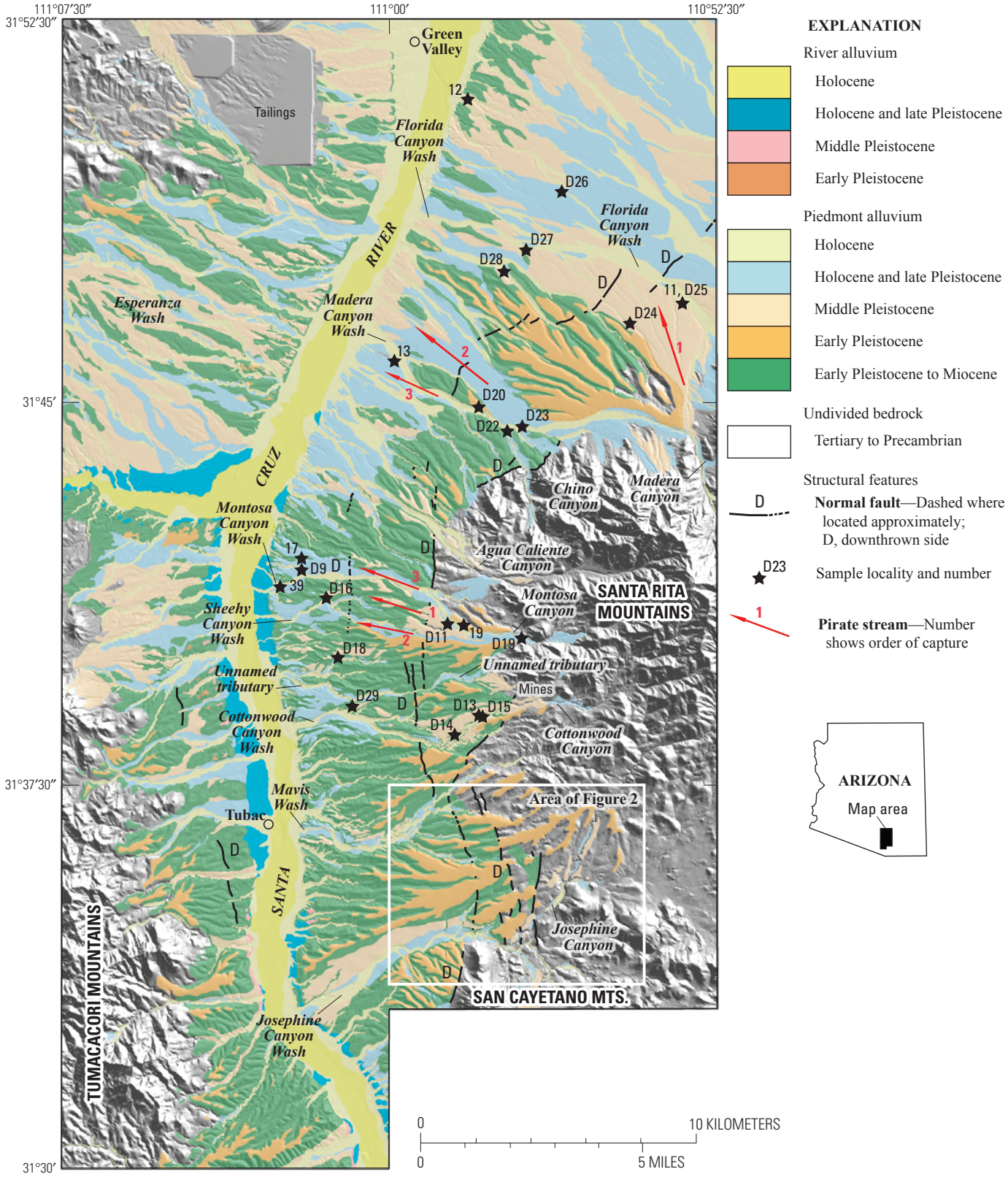

Figure 1. Generalized geology of upper Tertiary and Quaternary alluvium of the Santa Cruz River valley, Green Valley-Tubac area, Arizona (compiled from Lindsey and Van Gosen, 2006; Pearthree and Youberg, 2000; Spencer and others, 2003; and Youberg and Helmick, 2001); also shown are sample locations for this study, and area of figure 2. Individual samples (A, B, and so forth) in close vicinity are not shown. Shaded relief base by D.H. Knepper, Jr.

basins. Indeed, in this report we show that they are texturally similar to younger stream-terrace gravels.

During Pleistocene time, piedmont tributaries, such as Madera Canyon Wash, shifted course on the piedmont as they cut valleys in bedrock and basin fill. Changes in channel course were probably triggered by avulsion during storms and floods, but headward erosion of small tributaries set the stage for beheading and diversion. Stream capture is evident on Madera Canyon Wash and Montosa Canyon Wash. Study of geologic maps (Lindsey and Van Gosen, 2006; Pearthree and Youberg, 2000; Youberg and Helmick, 2001) readily reveals the probable sequence of stream piracy (fig. 1). The scenario of headward erosion and stream piracy outlined here differs from erosion on active alluvial fans, where streams exiting the mouths of mountain canyons cut channels into upper fan surfaces and transfer sediment onto lower fan surfaces (for example, Bull, 1964). Such fanhead trenches are recent features of active fan construction and are not to be confused with post-fan incision described here.

After deposition of basin fill during phase 1, the mountain front retreated as the predecessor of Madera Canyon Wash cut a surface on basin fill and granite and, in early Pleistocene time, deposited a thin (<20 m) gravel fan (fig. 1). Since then, piedmont streams adjacent to the Madera Canyon fan have captured and diverted the early Pleistocene Madera Canyon Wash. In middle Pleistocene time, Madera Canyon Wash flowed north from its mouth to join Florida Canyon Wash; the combined stream flowed northwest to join the Santa Cruz River. Capture was probably by a small tributary of Florida Canyon Wash that eroded southward along the base of the mountain front. During late Pleistocene time, a headward-eroding tributary of Chino Canyon Wash captured Madera Canyon Wash and diverted it along the south side of the early Pleistocene fan. Finally, during late Pleistocene or Holocene time, the lower part of Madera Canyon Wash was captured by a small tributary of the Santa Cruz River. Each of these events in the drainage history can be identified from the distribution of alluvial terraces (fig. 1).

Montosa Canyon Wash also cut a surface on basin fill and bedrock (including volcanic rocks) and, in early Pleistocene time, deposited a thin gravel fan (fig. 1). Like the early Pleistocene alluvium of the Madera Canyon fan, this deposit spreads radially from the canyon mouth, and also like the Madera Canyon fan, this deposit is not more than 10–20 m thick. The northern part of the early Pleistocene fan of Montosa Canyon Wash was dissected by a new, downcutting channel in middle Pleistocene time, which left a wide terrace fill on the order of 5 m thick. Headward-cutting Sheehy Canyon Wash appears to have captured the mountain reach of Montosa Canyon Wash in late Pleistocene time, only to lose it to a tributary that follows the piedmont course of Montosa Canyon Wash today. These events are recorded by the distribution of middle and late Pleistocene terrace deposits. Of interest also is the headcut of an unnamed tributary of the Santa Cruz River, which is now within 1 km southwest of Montosa Canyon Wash where it enters the piedmont. Perhaps the unnamed tributary will become the next piedmont course of Montosa Canyon Wash.

During middle Pleistocene time, the unnamed tributary drained some hills of carbonate rock (near “mines” in the southeast part of fig. 1), as indicated by a thin dissected pediment in its headwaters. A middle Pleistocene terrace near the tributary’s lower end (at sample locality D29, fig. 1) contains carbonate clasts that probably came from the area of the mines. The ancestral middle Pleistocene tributary flowed toward, and may have even joined, the downstream end of Cottonwood Canyon Wash.

In contrast to Madera Canyon and Montosa Canyon Washes, Cottonwood Canyon Wash appears to have followed the same course since middle Pleistocene time (fig. 1). Terraces of middle and late Pleistocene age occur along an approximately 25-m-deep canyon where downcutting proceeded faster than in adjacent tributaries. The mountain catchment basin of Cottonwood Canyon Wash has approximately the same bedrock geology, relief, and area as the basins of Madera Canyon Wash and Montosa Canyon Wash, but its bedrock is not as extensively faulted and fractured (table 1).

Josephine Canyon Wash (fig. 2) appears to follow the model of Cottonwood Canyon Wash—a permanent channel location since middle Pleistocene time and deep incision, especially in the lower (foothills) catchment. In addition, Josephine Canyon Wash has a larger upper (mountain) catchment basin than the others (table 1). The catchment basin is composed of two parts: an upper, mountain terrane of volcanic and plutonic rocks, and a lower, foothills terrain, still rugged but at lower elevation, composed of Tertiary volcanic and volcaniclastic sedimentary rocks (Drewes, 1971). Like Madera Canyon and Montosa Canyon Washes, Josephine Canyon Wash also spread a thin gravel fan over basin fill and bedrock during early Pleistocene time. The Josephine Canyon Wash fan extended upstream across the lower catchment basin with its apex immediately below the upper basin (fig. 2). Thus, the effective mountain catchment basin for the fan was 40 km^2. When the Josephine Canyon Wash fan was dissected in middle Pleistocene time, it provided the large volume of sediment that is now stored downstream in the depositional terrace (Qm, fig. 2) along the north side of present-day Josephine Canyon Wash. At points overlooking Josephine Canyon, middle Pleistocene terrace alluvium is as much as 18 m thick. During middle Pleistocene time, the wash followed a course immediately north of its present course.

The large depositional terrace of middle Pleistocene age that borders the north side of Josephine Canyon Wash was followed by formation of two lower erosional terraces of late Pleistocene and Holocene age (fig. 2). The bedrock horst of the San Cayetano Mountains may have been responsible for stabilizing the course of Josephine Canyon Wash during middle Pleistocene and later time. The high westernmost part of the San Cayetano Mountains is fault bounded (Lindsey and Van Gosen, 2006). The western fault boundary is readily visible and offsets early Pleistocene gravel that extends up to the mountain front. Although no northern boundary fault is

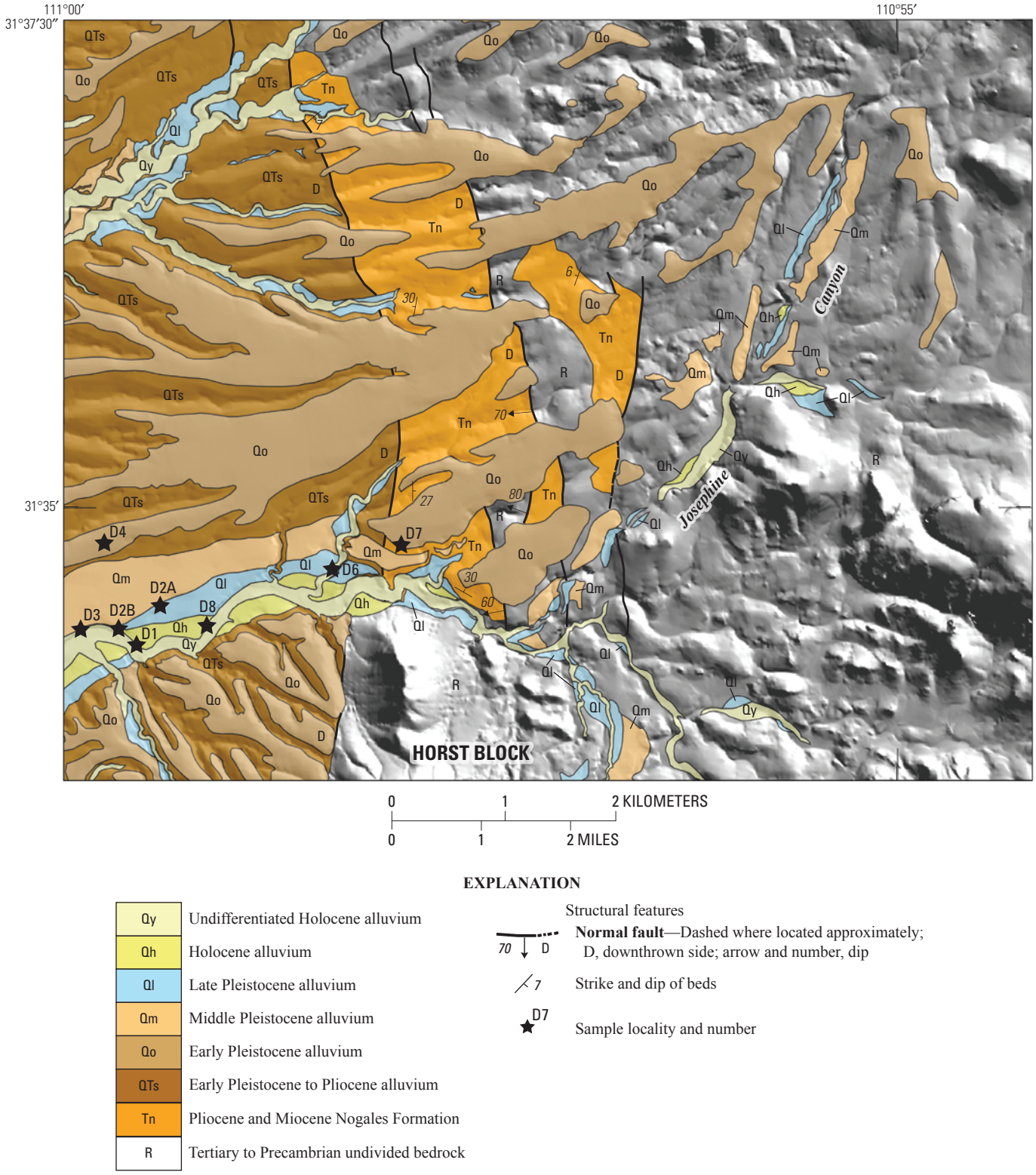

Figure 2. Details of upper Tertiary and Quaternary alluvium in the upper part of Josephine Canyon (from Lindsey and Van Gosen, 2006) and sample locations, Josephine Canyon Wash, Arizona. Shown separately are Miocene and Pliocene Nogales Formation (basin fill) and Holocene terrace deposits. Shaded relief base by D.H. Knepper, Jr.

Table 1. Comparison of mountain bedrock catchment basins: Madera Canyon Wash, Montosa Canyon Wash, Cottonwood Canyon Wash, and Josephine Canyon Wash, west slope of the Santa Rita Mountains, southeastern Arizona. All values are approximate.

[volc, volcanic rocks; plu, plutonic rocks, mainly granitic; sed, sedimentary rocks (estimated from Drewes, 1971)]

	Madera Canyon Wash	Montosa Canyon Wash	Cottonwood Canyon Wash	Josephine Canyon Wash
Mountain catchment area in km^2	19	9	14	100[1]
Maximum relief and (elevation) in m	1,540 (2,880)	1,320 (2,600)	1,320 (2,600)	1,780 (2,880)
Bedrock geology	volc=plu>>sed	plu>volc>sed	volc>plu>>sed	volc>plu>sed
Faulted structure	strong	strong	minor	moderate[2]

[1]Lower (foothills) catchment, 60 km^2; upper (mountain) catchment, 40 km^2.

[2]Faulted below Salerno fault; not faulted above fault (Drewes, 1971).

visible at the surface, it must underlie the young terrace gravel of the wash. The northward continuation of the west boundary fault is concealed where it is overlain by early Pleistocene fan gravel, indicating that the area located north of the wash had not been tectonically active while the San Cayetano Mountains horst continued to rise.

Terrace Classification and Formation

Terraces may be classified as erosional, in which the surface is underlain by thin lags of channel bedload, or as depositional, in which the surface is underlain by thick alluvial fill of channel and overbank deposits (Encyclopedia Britannica, 2010). Sometimes erosional terraces are called “strath terraces” or “degradational terraces,” and depositional terraces are called “fill terraces” or “aggradational terraces” (Bull, 1991). These terms can be confusing, in that erosional terraces represent periods of near-equilibrium—not downcutting—when streams cut laterally and leave behind a lag of channel gravel. The thickness of gravel deposits represents the depth of scour. The process of lateral cutting by migration of the stream channel is well illustrated on the middle reaches of Josephine Canyon Wash (fig. 3*A*). There, concave banks of meander bends undercut cliffs of soft gravel deposits of early Pleistocene and Pliocene age, whereas gravel accumulates along convex banks of meander bends. The wash is dry most of the time, but erosion and deposition occur during bankfull and higher flow. The gravel floodplain grows primarily by lateral accretion of bars to the bank. The floodplain surface has been stabilized by trees, shrubs, and grasses; only light scour and deposition of overbank fines occur during high flow. Bar and swale structure (Bull, 1991), visible on the Holocene terrace of Josephine Canyon Wash as well as the floodplain, may reflect an earlier braided channel or indicate continuing light scour and deposition on the floodplain surface.

Terrace formation is the product of alternate states of stream equilibrium and disequilibrium. Equilibrium is represented by no net channel incision or deposition, whereas disequilibrium is represented by degradation (downcutting) or aggradation (filling). Channel incision can be initiated if base level falls, one stream captures another, or the climate changes. Each period of incision is followed by lateral cutting of floodplains as the stream returns to equilibrium. Likewise, sediment may accumulate (aggrade) in channels and on floodplains if base level rises, a stream is beheaded, or the climate changes. Channel incision is well illustrated by the upper reaches of Josephine Canyon Wash (fig. 3*B*). There, the stream is actively downcutting into volcanic bedrock. During the late Pleistocene, the meandering stream cut laterally, forming a strath on bedrock. This stream was at near-equilibrium, like the middle reach is today. Meanders from the time of strath formation are now entrenched in bedrock; they reveal the planform of the former channel and the means by which it cut the strath. In contrast, channel filling is the dominant process on downstream reaches of Josephine Canyon Wash. Downstream, aggradation is revealed by a braided stream pattern where the stream is no longer able to transport its sediment load. Depositional terraces are often the product of braided streams.

Like Josephine Canyon Wash, most streams studied on the piedmont of the Santa Cruz River valley show the progression from degradation (incision upstream), equilibrium (meandering middle reach), to aggradation (braided downstream reach). Thus, both equilibrium and disequilibrium occur at the same time on different reaches (Bull, 1991; Schumm, 1993). As the incision-equilibrium-deposition cycle is repeated, terraces are formed when the floodplain is abandoned by renewed downcutting. Channel incision (or deposition) is only one possible response to change. Streams also adjust their gradient by changes in channel form (planform); channel form may be braided, meandering, or straight (Schumm, 1977, 1993). Often, as in the case of streams in the study area, these responses occur together.

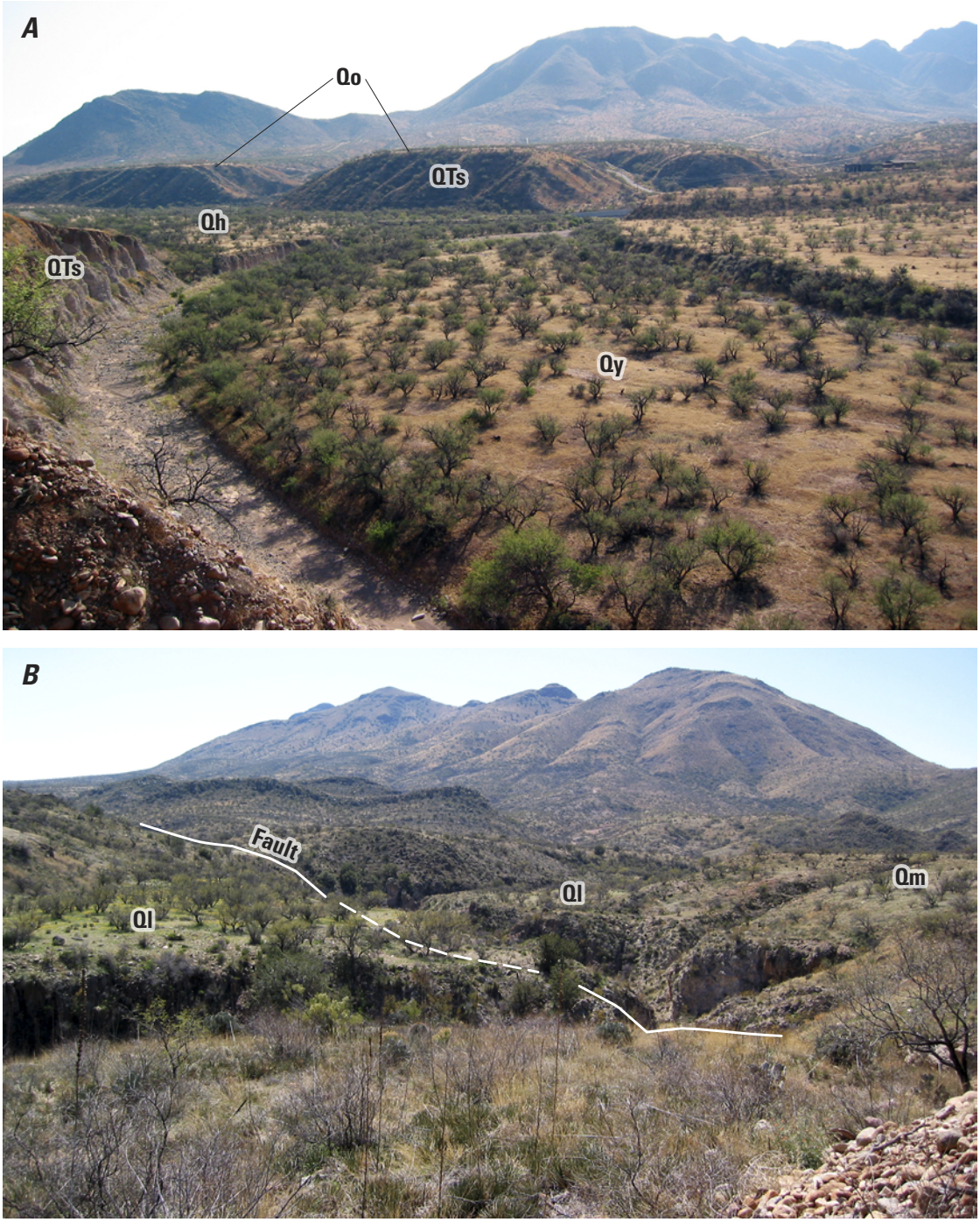

Figure 3. Formation of erosional terraces on Josephine Canyon Wash. *A*, View upstream (east) of the near-equilibrium middle reach (stream power/resisting power =1). The channel is undercutting outcrops (left side of photograph) of Pliocene to early Pleistocene alluvium (QTs) in concave meander bank. Modern floodplain (Qy) gravel accretes to convex meander bank in foreground. Vegetated floodplain surface shows bar and swale topography (Bull, 1991). Stepped terraces in background are of Holocene (Qh) and early Pleistocene (Qo) age; bedrock horst of the San Cayetano Mountains on skyline. *B*, View downstream (southwest) of the degradational upper reach (stream power/resisting power >1). The channel is confined to entrenched meanders in volcanic rocks as it continues to downcut. Meanders are probably inherited from the time when the late Pleistocene strath terrace (Ql) was cut. A normal fault crosses stream at the stream bend in the foreground, but does not offset the terrace, and continues in the bedrock saddle in the middle distance on left; high terrace on right side of photograph is of middle Pleistocene age (Qm); San Cayetano Mountains on skyline.

Degradation and aggradation can be understood by reference to Lane's (1955) equation for channel equilibrium:

$$Q_S \times D_{50} \propto Q_W \times S$$

where

Q_S is sediment discharge (supply or load),
D_{50} is median particle size,
Q_W is stream discharge (streamflow), and
S is channel slope.

When all four variables are in balance, the stream is in equilibrium, but when one or more variables change, the stream is in disequilibrium until other variables compensate. Depending on the direction of change, disequilibrium is revealed by degradation (incision, vertical cutting) or by aggradation (deposition). Equilibrium is indicated by lateral cutting. Channel incision is favored when stream power ($Q_W \times S$) exceeds resisting power ($Q_S \times D_{50}$); aggradation is favored when resisting power exceeds stream power (Bull, 1991). As illustrated for Josephine Canyon Wash, the downstream progression of stream power/resisting power of >1, =1, and <1 can be related to the progression from incision (>1, for upper reaches including tributaries) through equilibrium (=1, for middle reaches) to aggradation (<1, for lower reaches of the trunk stream).

Both theory and experiment indicate that the fundamental cause of lateral cutting of terrace surfaces is probably increased sediment supply (sediment discharge), although streamflow (stream discharge) plays a secondary role (Hancock and Anderson, 2002). Sediment supply and stream discharge are subject to rapid change and thus are the principal causes of disequilibrium. When sediment supply increases, streams deposit alluvium on their valley floors and cut laterally. The alluvial cover protects the valley floor from downcutting. When sediment supply wanes or streamflow increases, streams resume downcutting, leaving a terrace above the new channel.

As the master stream, the Santa Cruz River defines base level for its piedmont tributaries. During periods of downcutting by the river, base level drops, slopes increase at the foot of the piedmont, and tributary streams cut headward. During periods of river-valley filling, base level rises, and tributaries cut laterally, then aggrade (Schumm, 1993). In this scenario, the history of piedmont incision and terrace formation is linked to the base-level control of the Santa Cruz River. Base level of the Santa Cruz River may have dropped 50–80 m since middle Pleistocene time, based on the elevation of terrace remnants mapped on the west side of the river near Tubac (fig. 1) (Helmick, 1986; Youberg and Helmick, 2001). Between 8 and 5.6 ka, in Holocene time, the river alternated between downcutting and filling with little or no net decline in base level; this time period is interpreted to reflect arroyo cutting as desert vegetation replaced woodlands when the climate became warm and dry (Waters and Haynes, 2001). The effect of base-level change also depends upon the rate of change: slow changes would allow the river and its tributaries to remain in equilibrium through minor adjustments, such as changes in channel sinuosity (Schumm, 1993).

Faults that cross tributaries can create local base levels and alter stream slope. Rapid change, such as surface offset along faults that cross tributaries, creates knickpoints in the stream profile and has the potential to initiate incision upstream and aggradation downstream. However, at many places in the study area, faults mapped in basin fill have not moved since middle Pleistocene time, and in the area between Mavis Wash and Josephine Canyon Wash, there has been no fault movement since early Pleistocene time (figs. 1 and 2). Mapped evidence for late Pleistocene surface rupture is mostly north of Madera Canyon Wash. These constraints on the time of fault movement indicate tectonic stability during much of Pleistocene time, allowing hundreds of thousands of years for lateral cutting and for scarp retreat to the present mountain front.

Erosional embayments, pediments, and thin fans at canyon mouths also indicate tectonic stability (Bull, 1984). Except at the mouth of Chino Canyon, faults are not located at the mountain front, but instead are on the piedmont a few kilometers downstream (west) of the front. With the exception of Chino Canyon, the present mountain front is not a major fault boundary and is not straight, but instead consists of erosional embayments centered on canyon mouths. Rock-cut surfaces (pediments) beneath early Pleistocene gravels are observed on granite (Madera Canyon Wash) and volcanic rock (Montosa Canyon Wash) as well as on Nogales Formation (Josephine Canyon Wash, fig. 2). All of the surfaces cut on hard rock are on the upthrown sides of major valley fault systems and must represent a long expanse of time (fig. 1). These surfaces existed by early Pleistocene time, when thin fans were deposited at canyon mouths.

Profiles of ephemeral streams in southeastern Arizona reflect adjustment to tectonic stability during Quaternary time. These streams have concave-up profiles in mountain segments and nearly flat profiles in piedmont segments; they are adjusted to hydrologic factors, not base level (Cherkauer, 1972). Gradient, drainage area, and particle size follow channel profiles; all of these correlate with stream discharge. Steep mountain segments gather most of the stream discharge. Discharge increases very little or even diminishes downstream on narrow, elongate piedmont segments, as infiltration and evaporation remove as much discharge as is received from direct precipitation and overland flow (Cherkauer, 1972).

Under the stream-piracy scenario, a major wash emerging from the mountains may be captured by a minor wash within the basin, with opportunities for incision and aggradation on both streams (Ritter, 1987). Stream capture can also reorganize mountain catchment basins (Bull, 2009). In both basin and montane settings, a key factor is the relative elevation of the two streams; the capturing stream occupies a lower level than the stream it captures. On the piedmont, stream capture commonly takes place on the upper surfaces of alluvial fans, where a small wash located on the fan cuts headward and

captures the main wash draining the mountain catchment basin (Denny, 1967). As illustrated on the piedmont of the Santa Cruz River valley, the stage is set for stream piracy by headward-cutting washes on the flanks of early Pleistocene fans. The actual capture probably takes place by avulsion rather than headward erosion (Miller, 1959), when the higher, main wash overflows its banks and spills into the lower, small wash during an extreme event, such as a cloudburst.

Incision and aggradation after stream piracy can be profound (Bull, 2009). Capturing streams gain discharge and sediment supply; increased discharge results in incision and rapid headward erosion of the channel; whereas downstream, sediment will begin to accumulate. As incision wanes, aggradation proceeds upstream. Likewise, a stream beheaded by capture loses discharge and will begin to aggrade until its slope is sufficient to transport all of the available sediment.

Stream piracy has played an important role in dissection and terrace formation on the piedmont landscape of the Santa Cruz River valley since early Pleistocene time. Headward erosion by small washes on the upper piedmont diverted Madera Canyon Wash and Montosa Canyon Wash in middle and late Pleistocene time. Piracy and diversion of main washes to adjacent small washes terminated lateral cutting on the pirated stream. The valley of the pirated stream remained abandoned until some remnant or tributary of the pirated stream cut sufficiently headward to occupy it. In contrast, the pirate wash gained discharge and continued downcutting until increased sediment supply and decreased slope reestablished equilibrium, at which time it began to cut laterally and widen its valley. Washes that cut deeper canyons than Madera Canyon and Montosa Canyon, including Cottonwood Canyon Wash and Josephine Canyon Wash, do not show a record of stream piracy. Thus, terraces along Cottonwood Canyon and Josephine Canyon Washes did not form in response to stream piracy.

A hot, dry interglacial climate with monsoonal storm patterns, like those of today, and sparse desert vegetation might provide the conditions necessary to initiate erosion cycles that lead to lateral cutting of some reaches while degradation proceeds upstream and aggradation takes place downstream. Previous studies have linked aggradation in the lower Colorado River to interglacial periods, including the Holocene (Bull, 1991), when dry climate, sparse vegetation, and cloudbursts would have combined to increase sediment supply. However, short-term climate fluctuations within interglacial periods (see for example, Waters and Haynes, 2001) may complicate broad correlation of terrace formation with interglacials. A corollary of aggradation on the piedmont during dry periods is that stream incision is most likely to occur during cool, wet periods when vegetation was denser than the present, leading to higher stream discharge and lower sediment supply than the present (stream power/resisting power >1).

Terrace Deposits

Except near the mountain front, middle Pleistocene and younger terraces in the study area are mostly erosional; terrace surfaces are underlain by thin (commonly, 2–3 m) lag gravels (figs. 4*A*, 4*B*, and 4*C*). In contrast, fans of early Pleistocene age and a depositional terrace of middle Pleistocene age on Josephine Canyon Wash (figs. 5*A* and 5*B*) have thicknesses of 10–20 m. Near the mountain front, where abrupt changes in channel profile and dimensions cause streams to deposit their sediment load, terraces tend to be depositional. Older terrace gravel, of middle and early Pleistocene age, is deeply weathered, with the zone of red oxidation and rock disintegration extending into bedrock (fig. 4*C*). On the terrace surface, original channel topography is muted or absent. In contrast, younger (late Pleistocene and Holocene) terrace tops preserve bar-and-swale features (Bull, 1991).

Gravel in both erosional and depositional terraces of the study area always shows evidence of particle sorting and rearrangement by flowing water (figs. 4*B* and 6*A*, 6*B*, and 6*C*). In addition to weak layering in the form of lenses of varying particle size, common features include outsize clasts (such as boulders stranded by waning flow or lodged in finer sediment), clast clusters (clasts that lodge against one another during transport), and imbricate clusters (clasts resting on scour surfaces and rotated toward the upstream direction) (see Lindsey and others, 2005, for descriptions and references to these features in gravel deposits). These features are present in flash-flood deposits of perennial streams, but other evidence for perennial flow, such as clast-armor layers, downstream fining of gravel lenses, and crossbedding—all associated with gravel bars in perennial streams—is generally absent. Both layering and clast armor are absent or only weakly developed in gravel deposits of ephemeral streams in arid regions (Hassan, 2005; Laronne and others, 1994). The weak development of layering in most gravel deposits of piedmont tributary terraces of the Green Valley-Tubac area, and the absence of structures diagnostic of perennial streams, favors deposition in ephemeral streams with intermittent, flashy stream discharge.

Proximal deposits, that is, deposits formed near the mountain front, show evidence of both turbulent streamflood and debris-flow deposition in many regions (see for example, Bull, 1972; Costa, 1988; Blair and McPherson, 1994). Most proximal deposits studied here are of streamflood origin, but debris-flow origin cannot be excluded, because individual deposits may be transitional and criteria for distinction are not always clear. Proximal streamflood deposits below the mouth of Montosa Canyon are coarse and appear poorly sorted to the eye, but they contain crude stratification, lenses of imbricate clasts, possible horizons of clast armor, isolated large boulders, and clast clusters (figs. 6*A*, 6*B*, and 6*C*). All of these features are characteristic of streamfloods, and most or all can form during catastrophic floods (debris floods of Hungr, 2005;

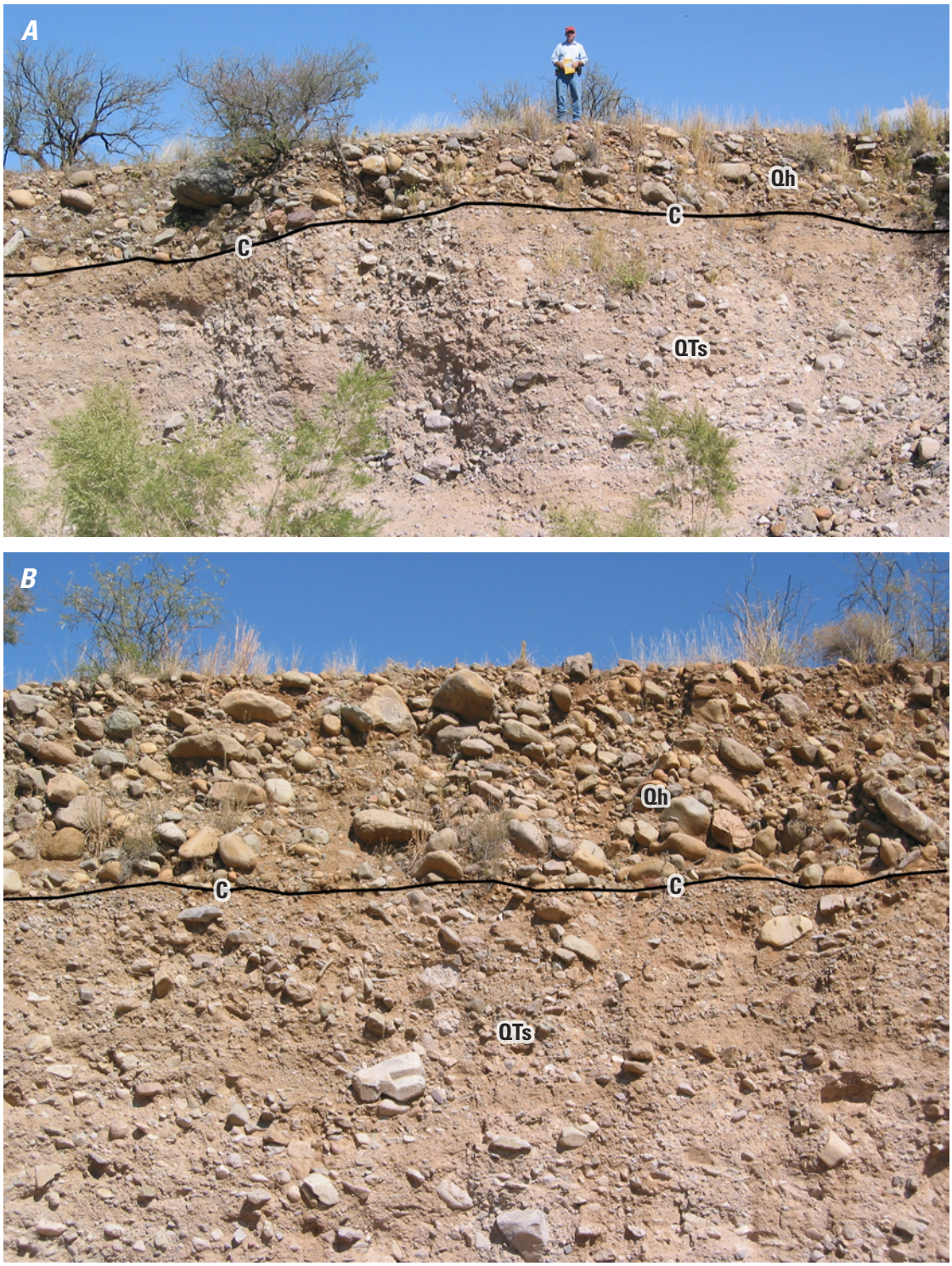

Figure 4. Erosional terraces. *A*, Erosional terrace of Holocene age (Qh) with thin gravel resting on Pliocene to early Pleistocene alluvium (QTs), north side Josephine Canyon Wash, sample locality D1 (fig. 2); C, units Qh-QTs contact. QTs outcrop in stream bank is too narrow to show on figure 2. *B*, Close view of figure 4*A*. Imbrication of large clasts is typical of streamflood deposits. Thin (2–3 m) terrace gravel deposits such as these represent the depth of scour and fill of former stream channels. *C*, Erosional terrace of middle Pleistocene age overlying basin fill (QTs), north side of Cottonwood Canyon Wash, sample locality D13 (fig. 1), showing weathered, clast-supported gravel, 3 m thick. Middle Pleistocene and older terrace deposits are deeply weathered, reddish in color, and surfaces are smooth.

Figure 4. Erosional terraces. *A*, Erosional terrace of Holocene age (Qh) with thin gravel resting on Pliocene to early Pleistocene alluvium (QTs), north side Josephine Canyon Wash, sample locality D1 (fig. 2); C, units Qh-QTs contact. QTs outcrop in stream bank is too narrow to show on figure 2. *B*, Close view of figure 4*A*. Imbrication of large clasts is typical of streamflood deposits. Thin (2–3 m) terrace gravel deposits such as these represent the depth of scour and fill of former stream channels. *C*, Erosional terrace of middle Pleistocene age overlying basin fill (QTs), north side of Cottonwood Canyon Wash, sample locality D13 (fig. 1), showing weathered, clast-supported gravel, 3 m thick. Middle Pleistocene and older terrace deposits are deeply weathered, reddish in color, and surfaces are smooth.—Continued

hyperconcentrated flows of Pierson, 2005). Stratification may be largely a product of aggradation, where successive floods have stacked layers on top of one another. Reverse grading and rafted clasts, a characteristic of debris flows where the largest boulders are concentrated near flow tops and fronts (see for example, Hungr, 2005), were observed only in early Pleistocene proximal deposits at Montosa Canyon Wash (fig. 6*B*). There, however, identification of rafted clasts on old terrace surfaces is uncertain because large boulders can be exposed by weathering and erosion of fine sediment. A single exposure of poorly sorted middle Pleistocene gravel, containing abundant interstitial sand and silt, in the banks of Florida Canyon Wash resembles a debris flow (fig. 6*D*), but interpretation is clouded by presence of faint stratification, imbrication in clast clusters, and a low Trask sorting coefficient.

Figure 5. Middle Pleistocene depositional terrace on Josephine Canyon Wash. *A*, Thick depositional terrace of middle Pleistocene age overlying Pliocene to early Pleistocene alluvium (QTs), north side Josephine Canyon Wash, sample locality D3 (fig. 2). Terrace gravel (Qm) is approximately 18 m thick. View is west, downstream. Unit QTs outcrop at base of cliff is too narrow to show on figure 2. *B*, Close view of figure 5*A* showing weak stratification and unconformable surface cut on Pliocene to early Pleistocene alluvium (QTs) (sample locality D3, fig. 2).

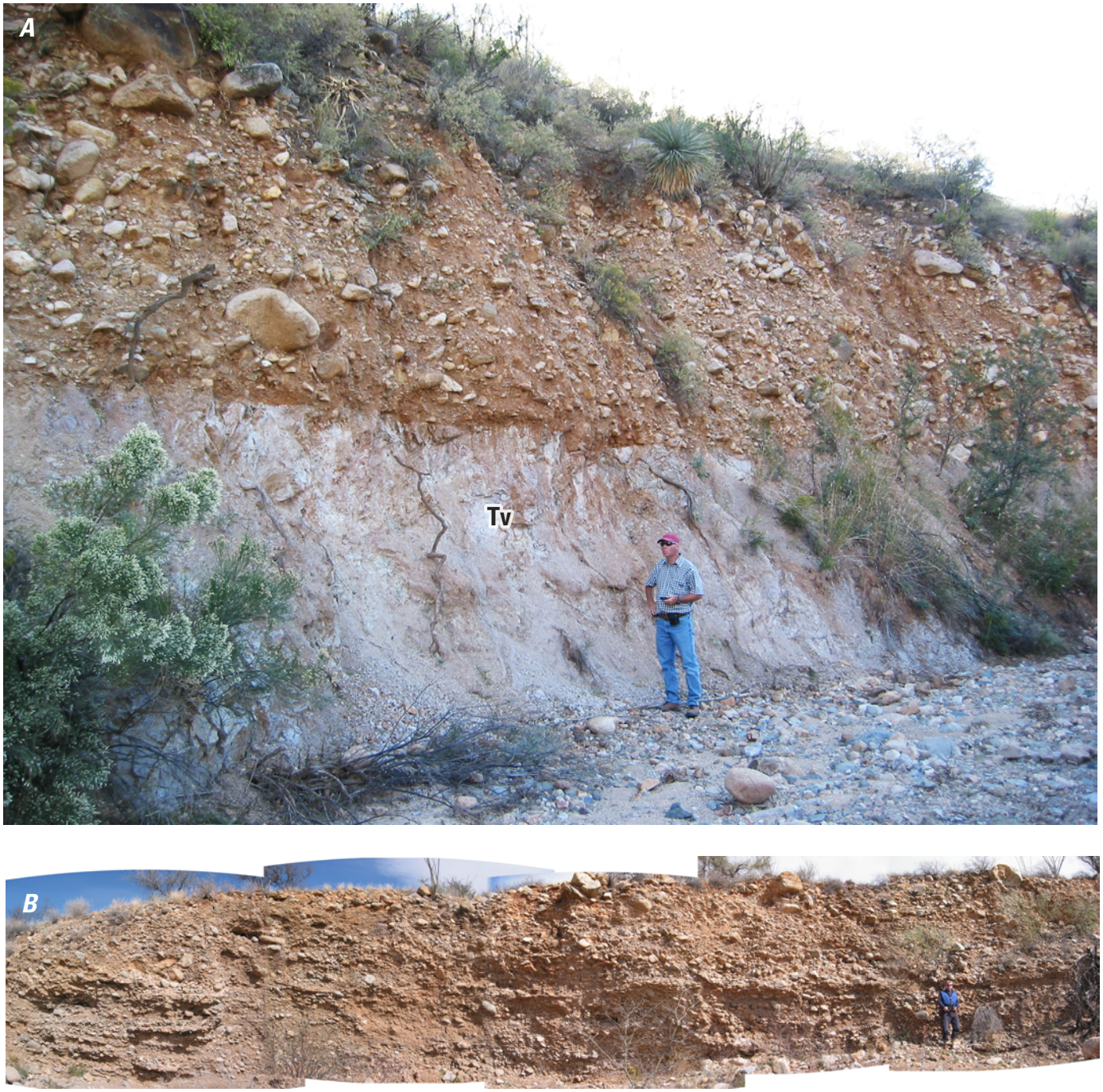

Figure 6. Sedimentary features in depositional terraces near the mountain front. *A*, Coarse terrace gravel of late Pleistocene age at the head of Montosa Canyon Wash, sample locality D19 (fig. 1), located near point where wash leaves the mountains at Whipple Observatory headquarters. Gravel was deposited on a smooth surface cut on volcanic rock (Tv). Note outsize boulders, upper left, and weak stratification. *B*, Panoramic view of fan gravel of early Pleistocene age on Montosa Canyon Wash, sample locality 19, about 1 km west of the mountain front. Stratified gravel deposited by repeated streamfloods. Large boulders on weathered surface may be remnants of a debris flow deposit, or may have been weathered out of coarse streamflood deposits. *C*, Close view, right side of figure 6*B*, showing stratification, imbrication (I), clast armor (A), outsize clasts (O), and clast clusters (CC) typical of streamflood deposits. Streamflow direction right to left. *D*, Middle Pleistocene terrace gravel interpreted as possible debris-flow deposit based on unsorted appearance, Florida Canyon Wash (sample locality 11, D25, fig. 1). However, the Trask sorting coefficient is in the range of streamflood deposits reported by Costa (1988). Also, note faint stratification, left center, and isolated imbricate cobble cluster between pack and boot, indicative of sorting. Photograph by Roger Melick.

Figure 6. Photographs of sedimentary features in depositional terraces near the mountain front. *A*, Coarse terrace gravel of late Pleistocene age at the head of Montosa Canyon Wash, sample locality D19 (fig. 1), located near point where wash leaves the mountains at Whipple Observatory headquarters. Gravel was deposited on a smooth surface cut on volcanic rock (Tv). Note outsize boulders, upper left, and weak stratification. *B*, Panoramic view of fan gravel of early Pleistocene age on Montosa Canyon Wash, sample locality 19, about 1 km west of the mountain front. Stratified gravel deposited by repeated streamfloods. Large boulders on weathered surface may be remnants of a debris flow deposit, or may have been weathered out of coarse streamflood deposits. *C*, Close view, right side of figure 6*B*, showing stratification, imbrication (I), clast armor (A), outsize clasts (O), and clast clusters (CC) typical of streamflood deposits. Streamflow direction right to left. *D*, Middle Pleistocene terrace gravel interpreted as possible debris-flow deposit based on unsorted appearance, Florida Canyon Wash (sample locality 11, D25, fig. 1). However, the Trask sorting coefficient is in the range of streamflood deposits reported by Costa (1988). Also, note faint stratification, left center, and isolated imbricate cobble cluster between pack and boot, indicative of sorting. Photograph by Roger Melick.—Continued

Gravel Lithology

Gravel lithology reflects the lithologic terrane of the catchment basin. As gravel is reworked downstream, it is redeposited with some modification of lithologic proportions, but the reworked gravel still reflects the distinctive lithologic composition of the catchment basin. Gravel lithology was determined by pebble counts below the catchment basins of Madera Canyon, Montosa Canyon, Cottonwood Canyon, and Josephine Canyon (fig. 7). Gravel on the piedmont below the mouth of Madera Canyon also contains contributions from Florida Canyon and Chino Canyon Washes that requires separate consideration (fig. 8). For this report, new data (appendix A, tables A1–A5) were combined with data from an earlier study (Lindsey and Melick, 2002). Details of methods and data are given in appendix A.

Granitic and volcanic rocks are abundant in terrace gravel from all four catchment basins, but the gravel of each basin is distinctive (fig. 7). Pebble counts show that gravel from Madera Canyon is distinguished by clasts of abundant granitic rocks and crystal-poor ignimbrite. Montosa Canyon gravel has conspicuous amounts of gabbro, diorite, carbonate rock, and quartz sandstone. Cottonwood Canyon and Josephine Canyon gravels have little or no gabbro, diorite, carbonate rock, or quartz sandstone; instead these gravels consist almost entirely of various granitic and volcanic rocks. As illustrated next, distinctive clasts and variations in lithologic proportions can be traced to specific catchment basins and help to identify previous positions of streams on the piedmont.

Gravel lithology is affected by drainage history on the piedmont, especially by capture and rerouting of major tributaries. For example, Madera Canyon Wash has followed several courses on the piedmont since it built a thin alluvial fan in early Pleistocene time, and each course had its own tributary system. During middle Pleistocene time, Madera Canyon Wash flowed directly north from the canyon mouth, where it was joined by Florida Canyon Wash, which still flows along the northern part of the early Pleistocene Madera Canyon fan. The middle Pleistocene gravel exposed in the banks of Florida Canyon Wash (sample 11, fig. 8) near the mountain front contains much more crystal-poor ignimbrite, more granitic rock, and no volcanics with quartz, unlike gravel derived only from Madera Canyon (samples D24A and D27, fig. 8). These differences reflect a major contribution from the mountain reaches of Florida Canyon, where granitic rocks of Precambrian age dominate (Drewes, 1980), and presumably, crystal-poor ignimbrite is abundant but other volcanics with quartz are not.

In late Pleistocene time, the Madera Canyon Wash flowed along the southern margin of the old alluvial fan, turning abruptly west at the mouth of the canyon and joining Chino Canyon Wash downstream. Chino Canyon Wash drains largely granitic terrane and joins Madera Canyon Wash on the piedmont about 8 km downstream from where the latter leaves the mountains. Gravel below the junction of Chino Canyon Wash and Madera Canyon Wash (sample 13, fig. 8) contains more granitic rock than terrace gravel on Madera Canyon Wash above the junction (sample D23). Thus, drainage history is reflected in gravel lithology. Abundant granitic-rock clasts in early Pleistocene gravel deposits (sample 20AB) below the modern junction reveal that Chino Canyon Wash has a long presence along the south side of the piedmont below Madera Canyon. The presence of abundant volcanic rocks with quartz suggests a contribution from early Pleistocene fan gravel, originally derived from Madera Canyon. During early Pleistocene time, a piedmont tributary of Chino Canyon Wash was already eroding the early Pleistocene Madera Canyon fan, but it did not capture the wash draining Madera Canyon until late Pleistocene time.

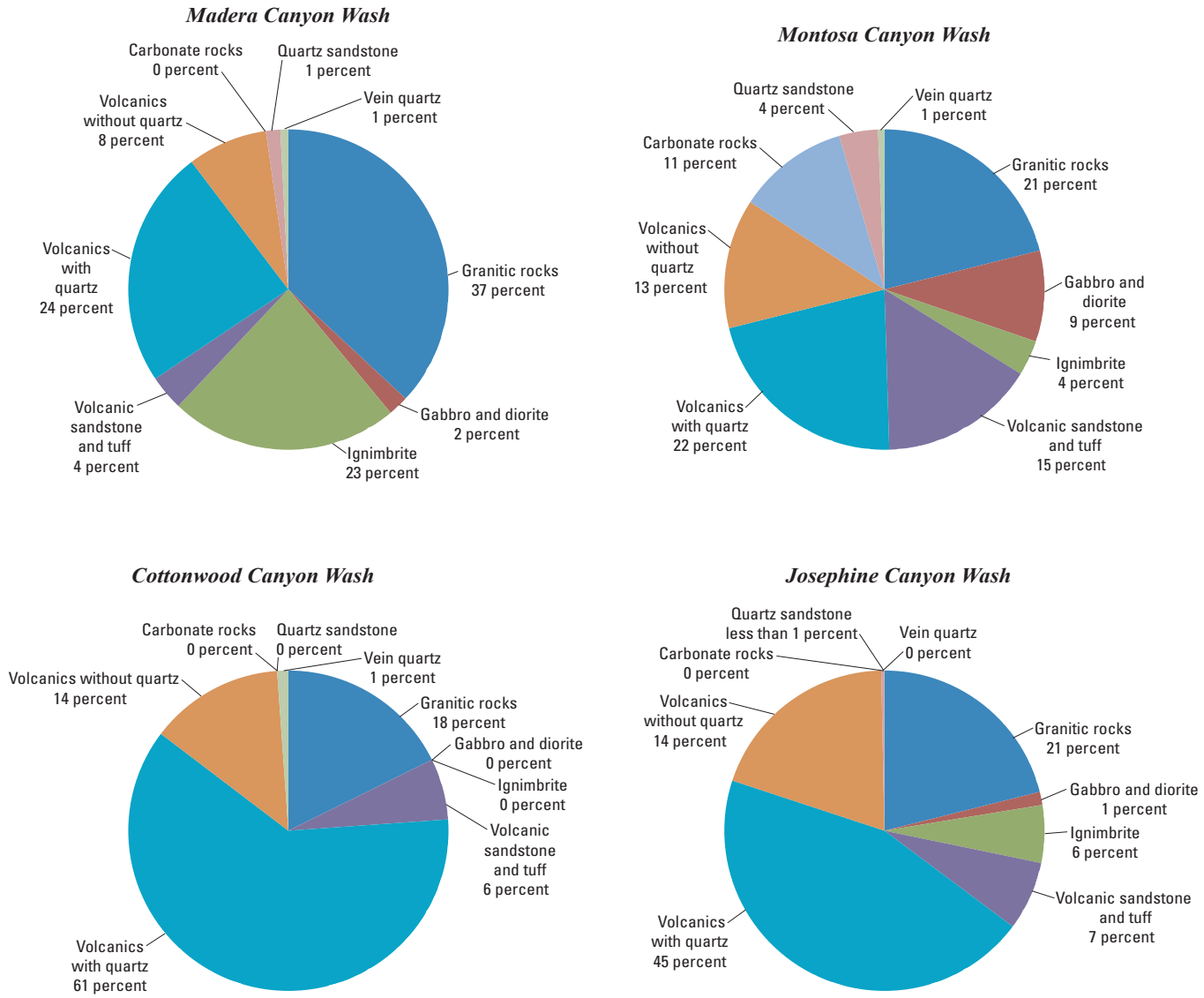

Figure 7. Summaries of clast lithology for early Pleistocene to Holocene gravel deposited by Madera Canyon Wash (600 pebbles), Montosa Canyon Wash (348 pebbles), Cottonwood Canyon Wash (101 pebbles), and Josephine Canyon Wash (561 pebbles). Gravels of Madera Canyon Wash include contributions from adjacent Florida Canyon Wash and Chino Canyon Wash (fig. 8).

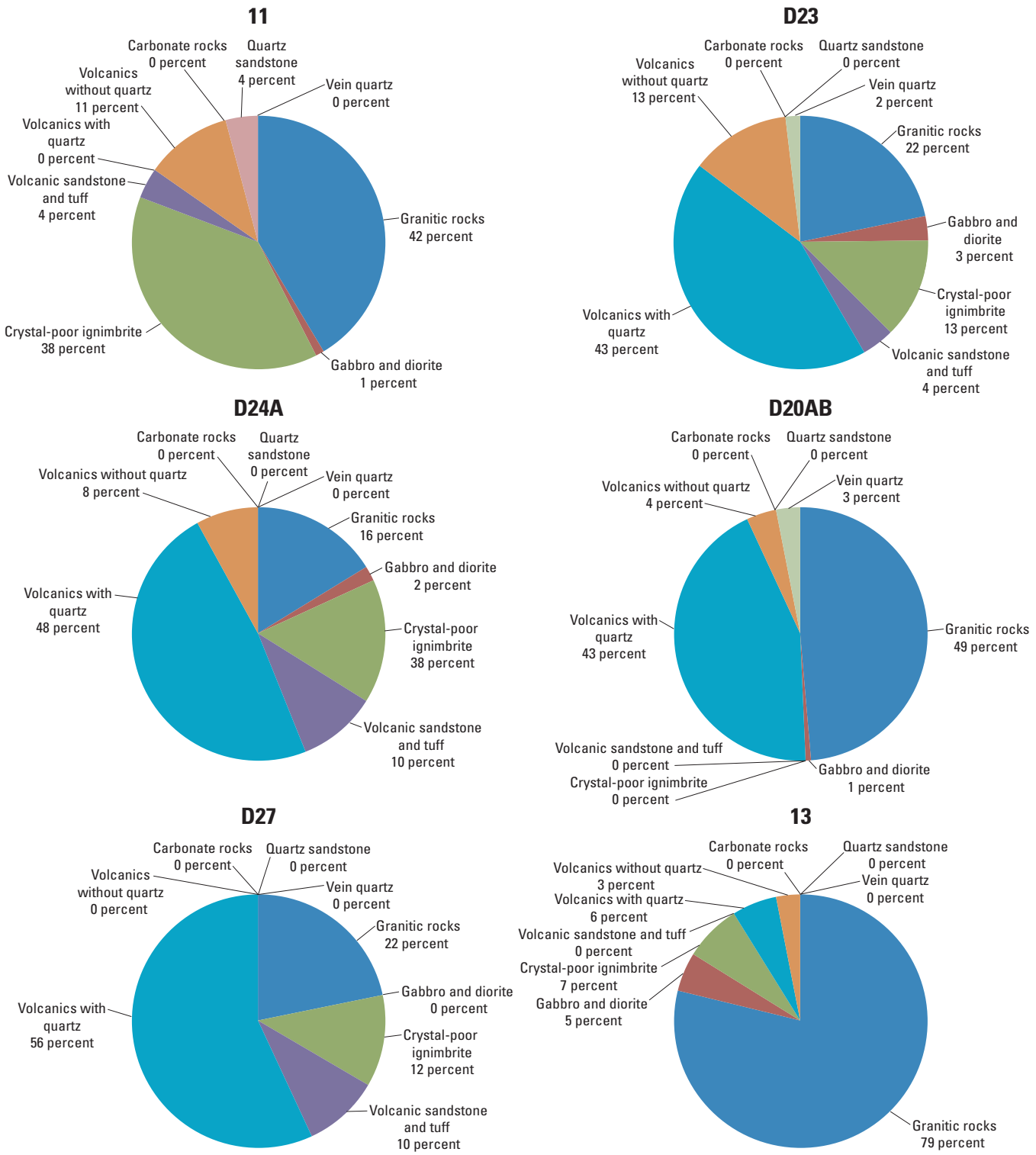

Figure 8. Summaries of clast lithology for gravel of Madera Canyon Wash as it changed course during Pleistocene time. Pie diagrams on left show terrace gravel, upstream (samples 11 and D24A) and downstream (sample D27), deposited by middle Pleistocene courses of the wash (fig. 1). Abundant granite and ignimbrite in the chart for sample 11 indicates a contribution from Florida Canyon Wash. Volcanics with quartz may be from Madera Canyon. Pie diagrams on right show late Pleistocene terrace gravel above (sample D23) and below (sample 13) junction with Chino Canyon Wash. Middle chart on right (sample D20AB) is early Pleistocene terrace gravel below junction with Chino Canyon Wash. Granitic rocks from Chino Canyon Wash are most abundant in gravel below the junction. Sample localities (fig. 1) are indicated by numbers or the letter "D" followed by a number; letters following locality numbers in figure 8 refer to samples taken at the same site.

Particle Size and Sorting

The particle size and sorting of gravel reflects downstream distance, stream competence, and transport and sorting mechanism. As with gravel lithology, our study of particle size focused on gravel deposited below Madera Canyon, Montosa Canyon, Cottonwood Canyon, and Josephine Canyon. For deposits on the north and south sides of the early Pleistocene Madera Canyon fan, particle size and sorting may reflect additional streamflow from Florida Canyon and Chino Canyon, respectively. Particle size was estimated by direct measurement along tape traverses on vertical outcrops of gravel instead of by sieving. Data are presented as cumulative frequency curves and statistics for quartiles and sorting. Methods, sample locations, data, and statistical computations are described in appendix B of this report. Sample localities are shown in figures 1 and 2.

Decreasing particle size downstream is well shown by comparing particle-size distributions for upstream and downstream locations of gravel deposited by Montosa Canyon Wash (figs. 9*A* and 9*B*) and the middle Pleistocene Madera Canyon Wash (figs. 10*A* and 10*B*). Other factors also influence particle size, and these can be illustrated by different terraces within the same reach—that is, where the downstream distance is approximately the same. Thin gravel of erosional terraces that overlie basin fill (QTs in fig. 1) is almost always coarser grained than basin fill (compare the particle-size curve for sample D24BU for Qh with that of D24BL for QTs in fig. 10*A*). The tendency for younger deposits to be coarse grained is also seen in early and late Pleistocene gravel along the present course of the Madera Canyon Wash (fig. 10*C*). The effect of transport mechanism is apparent from the slope of cumulative frequency distribution curves: a sample from gravel interpreted as a possible debris flow (sample D25B, fig. 10*D*) is flatter than clast-supported streamflow deposits (samples D25A and D25C, fig. 10*D*) at the same locality.

Perhaps the terrace gravels on Josephine Canyon Wash are the most striking example of the influence of continued reworking on particle size (fig. 11). The youngest (Qh and Ql in fig. 2), thinnest terrace deposits are the coarsest grained, and the oldest (Qo and Qm in fig. 2) and thickest deposits are the finest grained. When the old depositional terraces of Josephine Canyon Wash were eroded, fine sediment was winnowed and coarse particles were left as lags on newly formed erosional terraces. Particle size for all of the terrace gravels of the Josephine Canyon Wash was determined along a 3-km reach midway along the wash, about 5–8 km from the apex of the early Pleistocene Josephine Canyon fan and about 5–8 km upstream from the confluence with the Santa Cruz River (figs. 1 and 2).

The relation between deposit thickness and particle size and sorting was examined to search for criteria to distinguish depositional from erosional terrace deposits. Streams that are primarily aggradational, that is, they deposit sediment and raise their channel level, will form depositional terraces with thick fills. For example, the oldest and highest gravels (Qo and Qm, fig. 2) of Josephine Canyon are as much as 18–20 m thick; these are deposits of aggrading streams. Streams that are primarily degradational, that is, they cut down and during equilibrium, cut laterally, would be expected to form erosional terraces covered by thin, coarse lag deposits. For example, the young gravels (Ql and Qh, fig. 2) of Josephine Canyon are mostly 2–3 m thick but have larger median particle size than older terrace gravel; these are deposits of degrading streams that, when they reach equilibrium, cut laterally. Terrace steps record an overall history of degradation, but degradation may be punctuated by periods of lateral cutting during equilibrium or even by deposition during aggradation.

The deposits studied range from ≈2 m to as much as 20 m thick, but most are less than 12 m thick (fig. 12*A*). Within deposits <12 m thick, those ranging up to 6 m thick are interpreted as deposits of dominantly degradational streams. The thinnest (2–4 m thick) deposits may represent a single cycle of channel cutting and filling, followed by winnowing of fine grains, as reflected in larger overall particle size compared to nearby thick deposits (for example, Josephine Canyon, fig. 11). An intermediate class of deposits, 6–12 m thick, forms a “tail” on the primary mode of deposit thickness (fig. 12*A*). The intermediate class of deposits is not distinguishable by particle size or sorting from thin deposits on erosional terraces, but its greater thickness suggests some degree of aggradation by repeated deposition.

Most gravel deposits of Santa Cruz River tributaries are well sorted by the criteria of Trask (Krumbein and Pettijohn, 1938), having sorting coefficients (So) of less than 2.5. Sorting values compare well with those of streamflood deposits (water-flood deposits of Costa, 1988, who reported an average Trask sorting coefficient range of 1.8–2.7) and are well below values of debris-flow deposits (sorting coefficient range of 3.6–12.3, Costa, 1988). In this regard, the highest sorting coefficient (3.4) was calculated for the early Pleistocene gravel at sample locality 19 (fig. 1), in proximal deposits near the mouth of Montosa Canyon. The uppermost, weathered part of the fan gravel at locality 19 could be the remnant of a debris flow as indicated by large boulders on the surface (fig. 6*B*). However, the relatively high coefficient probably results from taking a composite sample of the entire outcrop, where lenses of both coarse and fine gravel are combined. Most of the gravel at sample locality 19 was deposited by streamflood, as indicated by stratification, imbrication, and sorting. In contrast, the deposit at locality 11 (figs. 1 and 6*D*; sample D25B, fig. 10*D*), interpreted as a possible debris flow, has a sorting coefficient of 2.4, well within the range of streamflood deposits.

A scatterplot of deposit thickness versus median particle size reveals little if any correlation between the two parameters (fig. 12*B*). Except for one anomalously thin measurement (locality D4, fig. 2), where the terrace surface has been eroded, thick aggradational deposits of early and middle Pleistocene age on Josephine Canyon (J on figs. 12*B* and 12*C*) plot in a separate field. Thickness versus median particle size of terrace deposits of other streams does not vary with age and does not

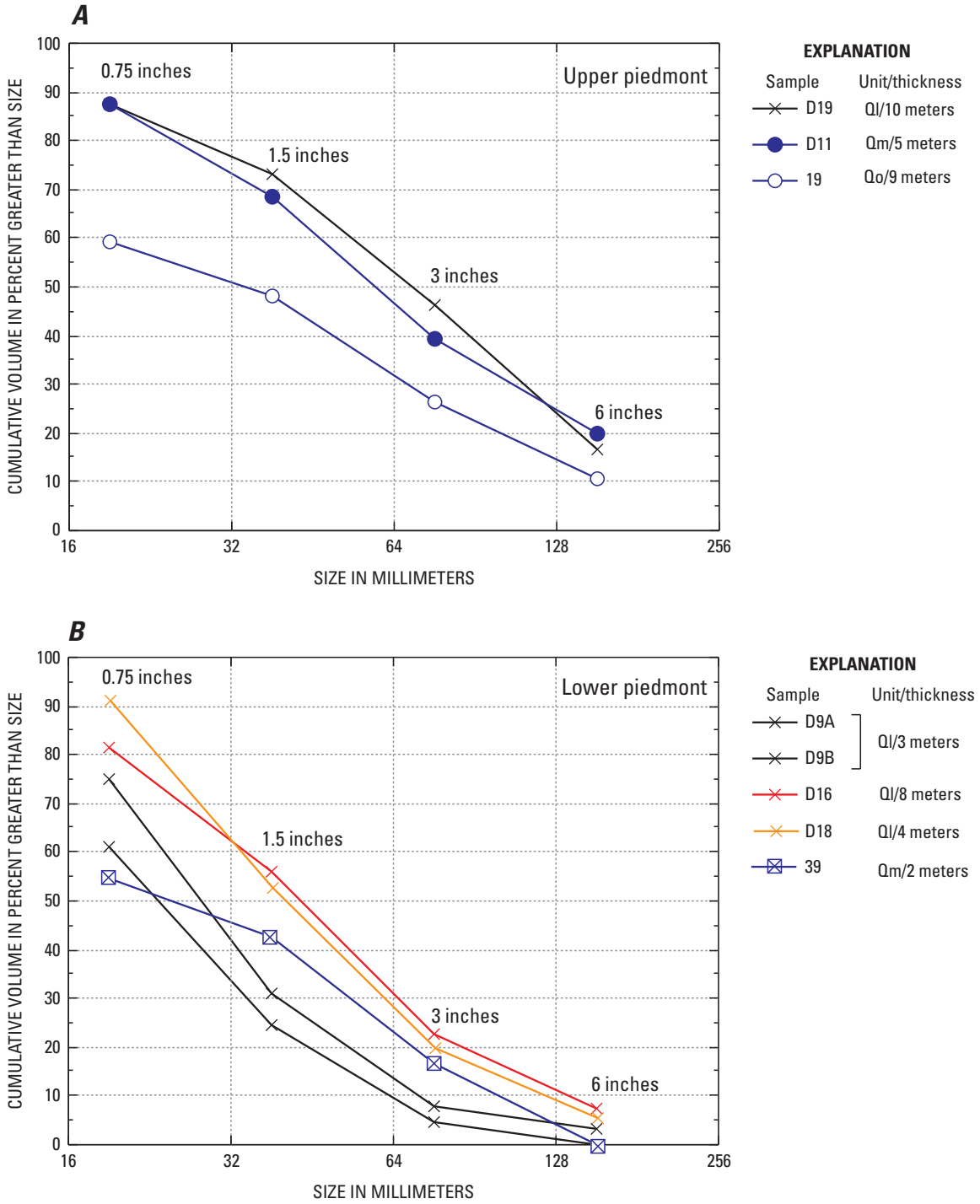

Figure 9. Cumulative frequency curves for particle size in gravel of varying age and distance from the canyon mouth of Montosa Canyon Wash. A, Upper piedmont; B, Lower piedmont. Sample localities in figure 1; exact locations and data in table B1.

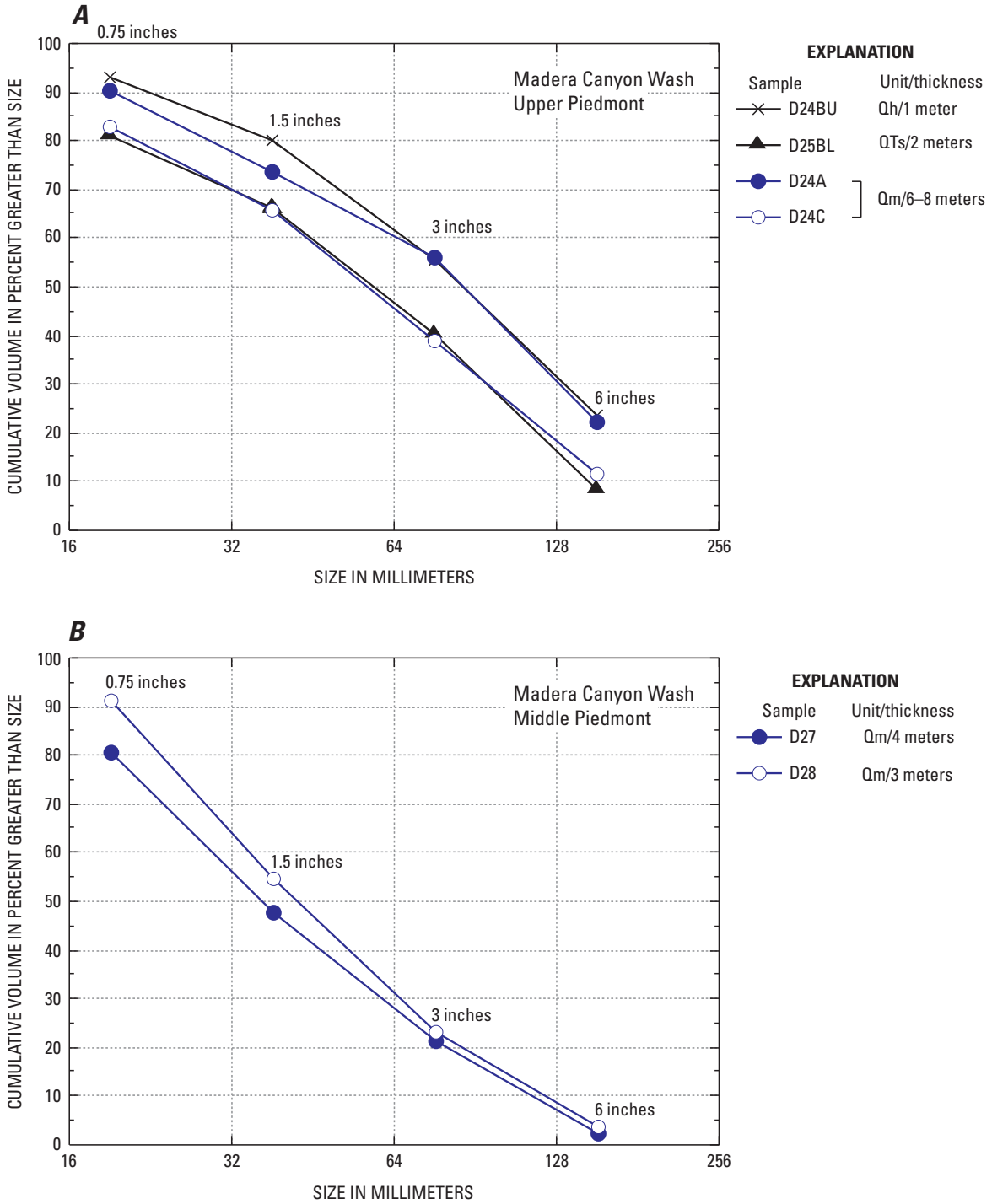

Figure 10. Cumulative frequency curves for particle size in gravel deposited by Madera Canyon Wash and Florida Canyon Wash. *A*, Gravel deposited on the upper part of middle Pleistocene Madera Canyon Wash (samples D24A and D24C. Also shown are samples D24BL and D24BU, of units QTs and Qh from the same location, to show the coarsening effect of reworking old fan gravel. *B*, Gravel from the midpoint (powerline road) of the middle Pleistocene Madera Canyon Wash (samples D27 and D28). *C*, Gravel deposited by the late Pleistocene (samples D22 and D23) and the early Pleistocene (samples D20A and D20B) Madera Canyon Wash. *D*, Gravel deposited by the middle Pleistocene Florida Canyon Wash and Madera Canyon Wash near their former junction (samples D25A, D25B, and D25C). The flat curve for sample D25B may reflect deposition by debris flow. Sample localities in figure 1; exact locations and data in table B1.

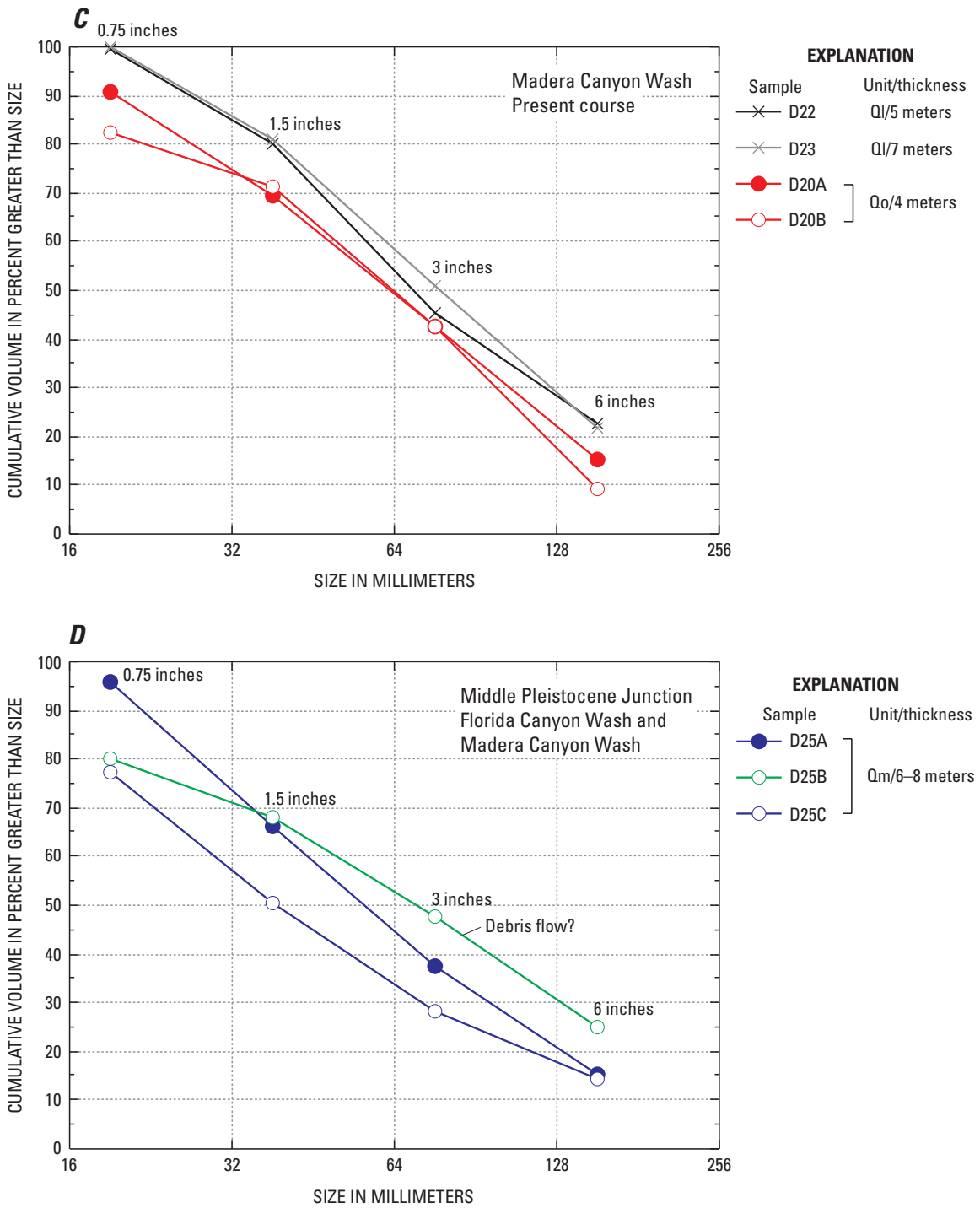

Figure 10. Cumulative frequency curves for particle size in gravel deposited by Madera Canyon Wash and Florida Canyon Wash. *A*, Gravel deposited on the upper part of middle Pleistocene Madera Canyon Wash (samples D24A and D24C. Also shown are samples D24BL and D24BU, of units QTs and Qh from the same location, to show the coarsening effect of reworking old fan gravel. *B*, Gravel from the midpoint (powerline road) of the middle Pleistocene Madera Canyon Wash (samples D27 and D28). *C*, Gravel deposited by the late Pleistocene (samples D22 and D23) and the early Pleistocene (samples D20A and D20B) Madera Canyon Wash. *D*, Gravel deposited by the middle Pleistocene Florida Canyon Wash and Madera Canyon Wash near their former junction (samples D25A, D25B, and D25C). The flat curve for sample D25B may reflect deposition by debris flow. Sample localities in figure 1; exact locations and data in table B1.—Continued

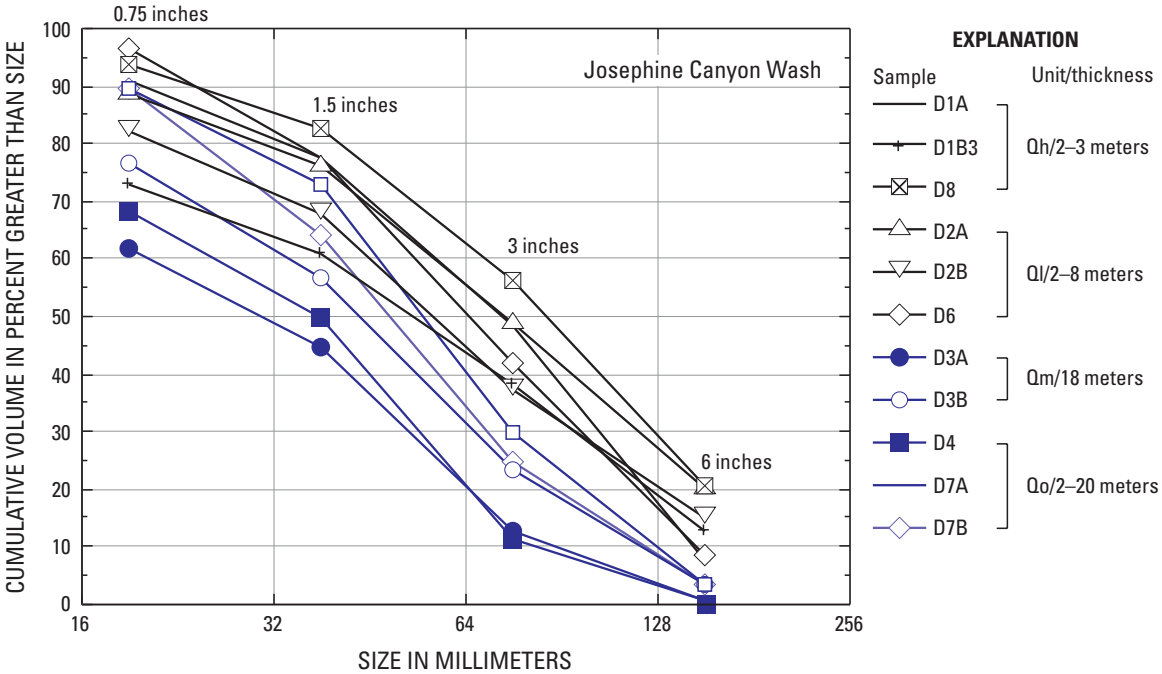

Figure 11. Cumulative frequency curves for particle size in gravel of varying age within a 3-km reach of Josephine Canyon Wash. Older, thicker gravel is finer grained than younger, thinner terrace gravel. Sample localities in figure 2; exact locations and data in table B1.

differ from terraces of late Pleistocene and Holocene age of Josephine Canyon. The confounding influence of distance from fan apex probably accounts for much of the variation in median particle size.

Terrace gravel of late Pleistocene age (and perhaps also of Holocene age) tends to be slightly better sorted (So <2) than deposits of older gravel (fig. 12*C*). Many well-sorted deposits of coarse terrace gravel are thin deposits on erosional terraces. Thus good sorting, coarse particle size, and thinness are the essential characteristics that distinguish erosional from aggradational terrace gravel. Aggradational terrace gravel (for example, the basin fill QTs, fig. 1) is often preserved in the geologic record.

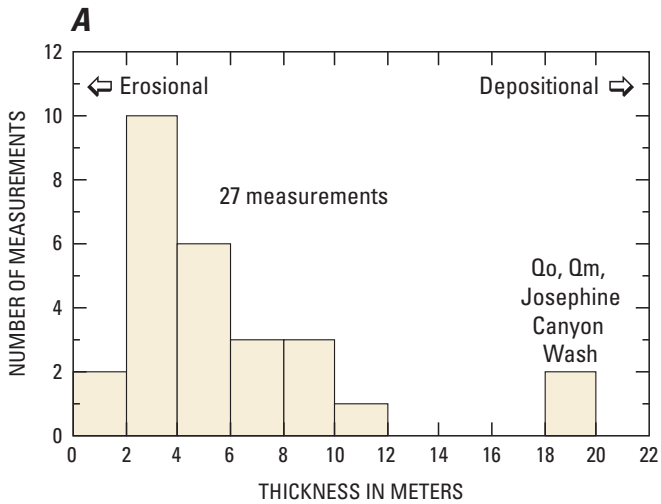

Figure 12. Thickness, sorting, and particle-size relations for terrace fill. *A*, Histogram of terrace thickness on the piedmont east of the Santa Cruz River, Green Valley-Tubac area. *B*, Scatterplot of terrace thickness versus median particle size. *C*, Scatterplot of sorting versus median particle size. High Trask sorting coefficients (So) indicate poor sorting; low coefficients indicate good sorting.

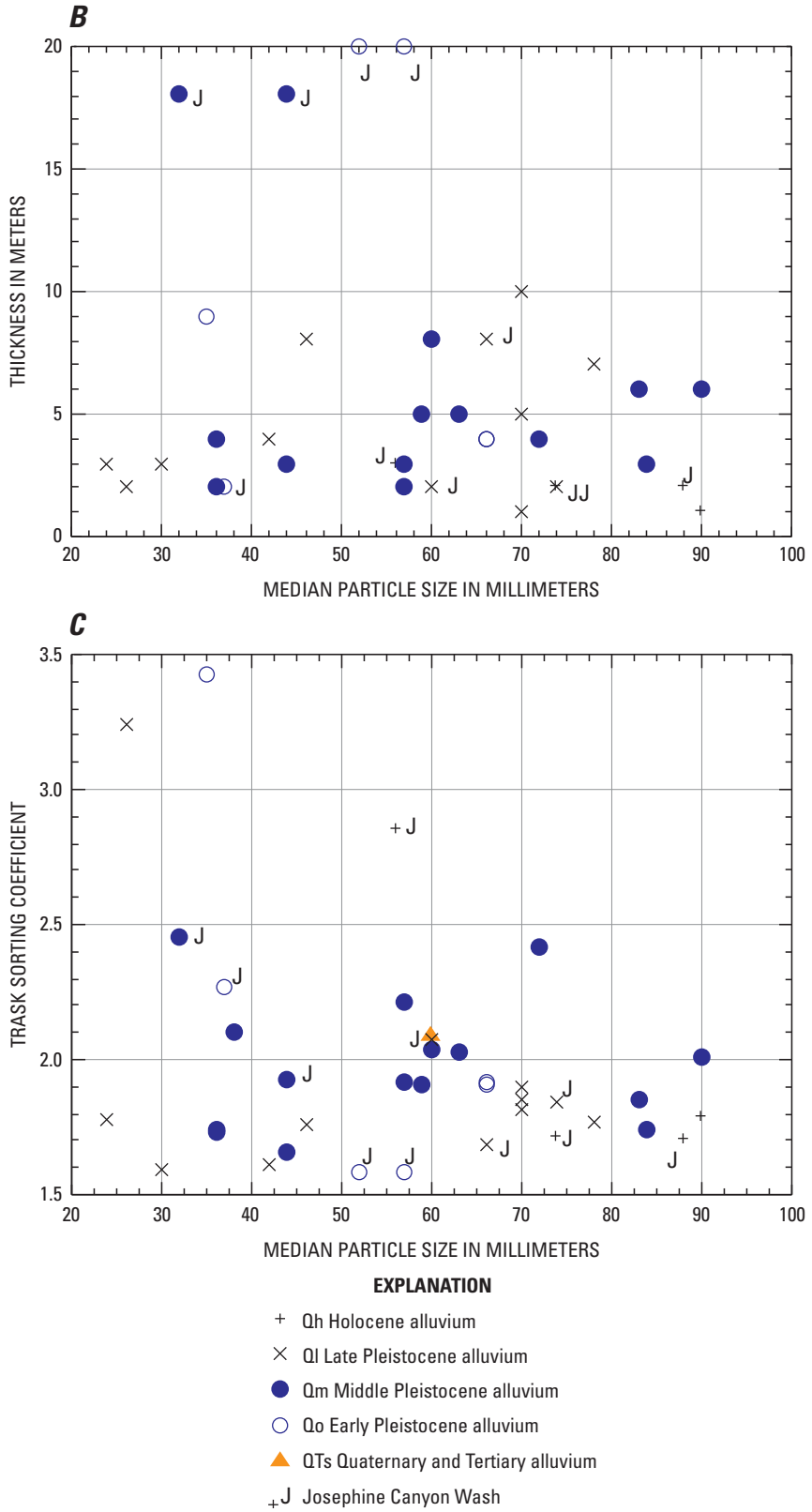

Figure 12. Thickness, sorting, and particle-size relations for terrace fill. *A*, Histogram of terrace thickness on the piedmont east of the Santa Cruz River, Green Valley-Tubac area. *B*, Scatterplot of terrace thickness versus median particle size. *C*, Scatterplot of sorting versus median particle size. High Trask sorting coefficients (So) indicate poor sorting; low coefficients indicate good sorting.—Continued

Discussion and Conclusions

Although canyon cutting on the piedmont defines the overall trajectory of landscape evolution on the Arizona piedmont, downcutting alternated with periods of lateral cutting that created the terraces of the present landscape. Lateral cutting was accompanied by deposition of thin deposits of coarse, well-sorted gravel that protect the terrace surface from erosion. Such thin gravel deposits have the sorting and sedimentary structures of streamflood deposits, replete with bar-and-swale surface topography on young examples; they represent the channel fill of the stream that cut the terrace. Examples of older gravel deposits, of middle Pleistocene age on Cottonwood Canyon Wash, are deeply weathered and do not preserve surface topography, but can be identified by their coarse particle size and good sorting as well as being only a few meters thick. All such terraces with thin gravel deposits are predominantly erosional in origin, the product of lateral cutting during periods of stream equilibrium.

In contrast to erosional terraces, gravel in depositional terraces is thicker (as much as 20+ m) and finer grained than their erosional counterparts in the same reach. Depositional terraces and fans near the mountain front may, however, contain exceptionally large boulders and, in some cases, are well-stratified. Depositional terrace gravels are primarily distinguished by evidence for rapid, repeated deposition—such as abundant fine sediment, poor sorting, and weakly developed bedding without deep scour surfaces—as well as by thickness. Depositional terraces are evidence of stream disequilibrium, when sediment supply overwhelmed the ability of the stream to move all of its bedload downstream.

The sedimentary features in terrace gravel of piedmont tributaries east of the Santa Cruz River are consistent with deposition by ephemeral streams in an arid environment. Trask sorting coefficients are typical of streamflood deposits, as are clast clusters and imbrication. Weakly developed bedding and general absence of clast armor are typical of ephemeral stream deposits (Laronne and others, 1994). Taken together, these features indicate deposition by flash floods in ephemeral streams under a desert climate like the present. In upstream reaches, where stream power exceeds resisting power, ephemeral streams downcut their mountain catchment basins and erode sediment. In middle reaches at near-equilibrium where stream power equals resisting power, streams cut laterally and leave a lag deposit equal to the depth of scour. Most of the sediment eroded from upstream passes through the middle reaches to be deposited downstream. In downstream reaches, where resisting power exceeds stream power, braiding and aggradation take place.

Evidence for deposition by debris flows is not supported by sedimentary features or low Trask sorting coefficients, but debris flows cannot be excluded for some proximal deposits below canyon mouths. Large boulders on terrace surfaces, weak development of bedding, and abundant matrix could be interpreted as evidence for debris flows or, alternatively, deposition by catastrophic floods. Likewise, the variety of flow processes and grain-size sorting in debris flows and related deposits (Hungr, 2005; Iverson, 2003) signals caution in excluding debris flows from interpretation of deposits near canyon mouths. Further investigation of the use of Trask sorting coefficients in describing the range of debris-flow sorting is also needed.

Changes in sediment supply and stream discharge are the underlying causes of terrace cutting (Hancock and Anderson, 2002). Increased stream discharge initiates downcutting, which decreases slope and leads to lateral cutting. Increased sediment supply interrupts downcutting and causes streams to cut laterally. In an arid climate, sparse vegetation and flashy discharge combine to increase sediment supply. For the drainages studied, sediment supply was not sufficient to promote long-term aggradation. Thus, except near the mountain front, streams cut erosional terraces. Only the middle Pleistocene Josephine Canyon Wash formed a depositional terrace downstream from the mountain front.

The 18-m-thick depositional terrace of middle Pleistocene age on Josephine Canyon Wash does not have counterparts on the other tributaries studied. In comparison, the extensive middle Pleistocene terrace of Cottonwood Canyon Wash is distinctly erosional in character, measuring no more than 2–3 m thick at two localities and 6 m thick a little farther upstream. The wide expanse of both terraces suggests an extended period of lateral cutting, but the thick fill of the Josephine Canyon terrace indicates that lateral cutting was followed by aggradation. Although temporal equivalence is not implied, these two contrasting terraces of middle Pleistocene age represent different responses by adjacent drainages. After lateral cutting, the sediment load of Josephine Canyon Wash remained high compared to that of Cottonwood Canyon Wash. The explanation for contrasting responses may be differences in size and geology of the catchment areas of the drainage basins (table 1). Much of the lower part of the large catchment basin of Josephine Canyon Wash is underlain predominantly by Tertiary volcanic and volcaniclastic sedimentary rock, and the lower basin was once covered by easily eroded early Pleistocene fan alluvium. These easily eroded rocks and sediments provided the fill for the middle Pleistocene depositional terrace downstream. In contrast, hard bedrock underlies the small catchment basin of Cottonwood Canyon Wash, and no large volume of easily eroded fan alluvium accumulated near the mountain front.

On tectonically stable landscapes like the piedmont of southeastern Arizona, cycles of terrace formation may represent either climate change or piracy. On Madera Canyon Wash and Montosa Canyon Wash, stream piracy initiated terrace formation through changes in stream discharge and sediment supply. On Cottonwood Canyon Wash and Josephine Canyon Wash, only climate change could have initiated terrace formation.

Evidence that adjacent streams have different histories of downcutting and terrace formation, in response to piracy or adjustment to catchment drainages of varying size and bedrock

composition, calls into question the assumption that terraces of adjacent tributaries are age equivalent. Classification of terraces according to weathering and soil development gives a general idea of age but does not establish age equivalence. Studies aimed at assessing links between terrace formation and climate change should focus on large tributaries with well-understood drainage histories.

References Cited

Blair, T.C., and McPherson, J.G., 1994, Alluvial fan processes and forms, *in* Abrahams, A.D., and Parson, A.J., eds., Geomorphology of desert environments: London, Chapman & Hall, p. 354–402.

Bull, W.B., 1964, Geomorphology of segmented alluvial fans in western Fresno County, California: U.S. Geological Survey Professional Paper 352–E, p. 87–129.

Bull, W.B., 1972, Recognition of alluvial-fan deposits in the stratigraphic record, *in* Rigby, J.K., and Hamblin, W.K., eds., Recognition of ancient sedimentary environments: Society of Economic Paleontologists and Mineralogists Special Publication 16, p. 63–83.

Bull, W.B., 1984, Tectonic geomorphology: Journal of Geological Education, v. 32, p. 310–324.

Bull, W.B., 1991, Geomorphic responses to climatic change: New York, Oxford University Press, 326 p.

Bull, W.B., 2009, Tectonically active landscapes: Chichester, United Kingdom, Wiley-Blackwell, 326 p.

Cherkauer, D.S., 1972, Longitudinal profiles of ephemeral streams in southeastern Arizona: Geological Society of America Bulletin, v. 83, no. 2, p. 353–366.

Connell, S.D., Hawley, J.W., and Love, D.W., 2005, Late Cenozoic drainage development in the southeastern basin and range of New Mexico, southeasternmost Arizona, and western Texas, *in* Lucas, S.G., Morgan, G.S., and Zeiler, K.E., eds., New Mexico's ice ages: New Mexico Museum of National History and Science Bulletin No. 28, p. 125–150.

Costa, J.E., 1988, Rheologic, geomorphic, and sedimentologic differentiation of water floods, hyperconcentrated flows, and debris flows, *in* Baker, V.R., Kochel, R.C., and Patton, P.C., eds., Flood Geomorphology: New York, Wiley-Interscience, 503 p.

Davis, O.K., 1999, Pollen and other microfossils in Pleistocene speleothems, Kartchner Caverns: Journal of Cave and Karst Studies, v. 61, no. 2, p. 89–92.

Denny, C.S., 1967, Fans and pediments: American Journal of Science, v. 265, no. 2, p. 81–105.

Drewes, Harald, 1971, Geologic map of the Mount Wrightson quadrangle, southeast of Tucson, Santa Cruz and Pima Counties, Arizona: U.S. Geological Survey Miscellaneous Investigations Series Map I–614, scale 1:48,000.

Drewes, Harald, 1980, Tectonic map of southeast Arizona: U.S. Geological Survey Miscellaneous Investigations Series Map I–1109, scale 1:125,000.

Encyclopedia Britannica, 2010, River terraces: Britannica Online Encyclopedia, unpaginated, accessed February 1, 2010, at *http://www.britannica.com/EBchecked/topic/504801/river/29110/River-terraces.*

Field, J.J., 1994, Surficial processes on two fluvially dominated alluvial fans in Arizona: Arizona Geological Survey Open-File Report 94–12, 31 p.

Gettings, M.E., and Houser, B.B., 1997, Basin geology of the upper Santa Cruz valley, Pima and Santa Cruz Counties, southeastern Arizona: U.S. Geological Survey Open-File Report 97–676, 40 p.

Hancock, G.S., and Anderson, R.S., 2002, Numerical modeling of fluvial strath-terrace formation in response to oscillating climate: Geological Society of America Bulletin, v. 114, no. 9, p. 1131–1142.

Hassan, M.A., 2005, Characteristics of gravel bars in ephemeral streams: Journal of Sedimentary Research, v. 75, no. 1, p. 29–42.

Helmick, W.R., 1986, The Santa Cruz River terraces near Tubac, Santa Cruz County, Arizona: Tucson, University of Arizona, M.S. thesis, 96 p.

Houser, B.B., Peters, L., Esser, R.P., and Gettings, M.E., 2004, Stratigraphy and tectonic history of the Tucson basin, Pima County, Arizona, based on the Exxon State (32)-1 well: U.S. Geological Survey Scientific Investigations Report 2004–5076, 37 p.

Hungr, O., 2005, Classification and terminology, *in* Jakob, M., and Hungr, O., eds., Debris-flow hazards and related phenomena: Berlin, Springer-Verlag, p. 9–23.

Iverson, R.M., 2003, The debris-flow rheology myth, *in* Rickenmann, D., and Chen, C.L., eds., Debris-flow hazards mitigation: mechanics, prediction, and assessment (v. 1): Rotterdam, Millpress, p. 303–314.

Klawon, J.E., and Pearthree, P.A., 2000, Field guide to a dynamic distributary drainage system—Tiger Wash, western Arizona: Arizona Geological Survey Open-File Report 00-01, 34 p.

Knepper, D.H., Jr., 2005, Bedrock erosion surface beneath the Rocky Flats alluvial fan, Jefferson and Boulder Counties, Colorado: Mountain Geologist, v. 42, no. 1, p. 1–8.

Krumbein, W.C., and Pettijohn, F.J., 1938, Manual of sedimentary petrography: New York, Appleton-Century-Crofts, 549 p.

Lane, E.W., 1955, The importance of fluvial morphology in hydraulic engineering: Proceedings of the American Society of Civil Engineers, v. 81, no. 745, p. 1–17.

Larrone, J.B., Reid, I., Yitshak, Y., and Frostick, L.E., 1994, The non-layering of gravel streambeds under ephemeral flood regimes: Journal of Hydrology, v. 59, no. 2, p. 353–363.

Leopold, L.B., Wolman, M.G., and Miller, J.P., 1964, Fluvial processes in geomorphology: San Francisco, Freeman, 522 p.

Lindsey, D.A., Langer, W.H., and Knepper, D.H., Jr., 2005, Stratigraphy, lithology, and sedimentary features of Quaternary alluvial deposits of the South Platte River and some of its tributaries east of the Front Range, Colorado: U.S. Geological Survey Professional Paper 1705, 70 p.

Lindsey, D.A., Langer, W.H., and Van Gosen, B.S., 2007, Using pebble lithology and roundness to interpret gravel provenance in piedmont fluvial systems of the Rocky Mountains, USA: Sedimentary Geology, v. 199, p. 223–232.

Lindsey, D.A., and Melick, Roger, 2002, Reconnaissance of alluvial fans as potential sources of gravel aggregate, Santa Cruz River valley, southeast Arizona: U.S. Geological Survey Open-File Report 02–314, 46 p.

Lindsey, D.A., and Van Gosen, B.S., 2006, Surficial geologic map of the Mount Hopkins and northern part of the San Cayetano Mountains 7.5′ quadrangles, Santa Cruz and Pima Counties, Arizona: Arizona Geological Survey Contributed Map 06–A (CM-06-A), 1 sheet, scale 1:24,000.

Melton, M.A., 1965, The geomorphic and paleoclimatic significance of alluvial deposits in southern Arizona: Journal of Geology, v. 73, no. 1, p. 1–38.

Menges, C.M., and McFadden, L.D., 1981, Evidence for a latest Miocene to Pliocene transition from basin-range tectonic to post-tectonic landscape evolution in southeastern Arizona: Arizona Geological Society Digest, v. 13, p. 151–160.

Menges, C.M., and Pearthree, P.A., 1989, Late Cenozoic tectonism in Arizona and its impact on regional landscape evolution, *in* Jenny, J.P., and Reynolds, S.J., eds., Geologic evolution of Arizona: Arizona Geological Society Digest, v. 17, p. 649–680.

Miller, J.P., 1959, Geomorphology in North America: Przeglad Geograficzny, v. 31, no. 3–4, p. 567–587.

Pearthree, P.A., and Youberg, Ann, 2000, Surficial geologic maps and geologic hazards of the Green Valley-Sahuarita area, Pima County, Arizona: Arizona Geological Survey Open-File Report 00–13, scale 1:24,000, text 21 p.

Pearthree, P.A., and Youberg, Ann, 2006, Recent debris flows and floods in southeast Arizona: Arizona Geology, v. 36, no. 3, 6 p.

Pettijohn, F.J., 1975, Sedimentary rocks (3rd ed.): New York, Harper and Row, 628 p.

Pierson, T.C., 2005, Hyperconcentrated flow—Transitional process between water flow and debris flow, *in* Jakob, M., and Hungr, O., eds., Debris-flow hazards and related phenomena: Berlin, Springer-Verlag, p. 159–202.

Ritter, D.F., 1987, Fluvial processes in the mountains and intermontane basins, *in* Madole, R.F., Bradley, W.C., Loewenherz, D.S., Ritter, D.F., Rutter, N.W., and Thorn, C.E., chap. 7 *of* Graf, W.L., ed., Geomorphic systems of North America: Boulder, Colo., Geological Society of America, Centennial Special Volume 2, p. 220–228.

Schumm, S.A., 1977, The fluvial system: New York, Wiley, 338 p.

Schumm, S.A., 1993, River response to baselevel change—Implications for sequence stratigraphy: Journal of Geology, v. 101, no. 2, p. 279–294.

Simons, F.S., 1974, Geologic map and sections of the Nogales and Lochiel quadrangles, Santa Cruz County, Arizona: U.S. Geological Survey Miscellaneous Investigations Series Map I–762, scale 1:48,000.

Spencer, J.E., Ferguson, C.A., Richard, S.M., and Youberg, A., 2003, Geologic map of the Esperanza Mill 7.5′ quadrangle, Pima County, Arizona: Arizona Geological Survey Digital Geologic Map DGM–33, scale 1:24,000, text 10 p.

Thompson, R.S., Shafer, S.L., Strickland, L.E., Van de Water, P.K., and Anderson, K.H., 2003, Quaternary vegetation and climate change in the Western United States—Developments, perspectives, and prospects, *in* Gillespie, A.R., Porter, S.C., and Atwater, B.F., eds., The Quaternary Period in the United States—Developments in Quaternary science, v. 1: Amsterdam, Elsevier, p. 403–426.

Waters, M.R., and Haynes, C.V., 2001, Late Quaternary arroyo formation and climate change in the American Southwest: Geology, v. 29, no. 5, p. 399–402.

Youberg, A., and Helmick, W.R., 2001, Surficial geologic maps and geologic hazards of the Amado-Tubac area, Santa Cruz and southern Pima Counties, Arizona: Arizona Geological Survey Digital Geologic Map 13, scale 1:24,000.

Appendixes

Appendix A. Pebble Lithology and Roundness Counts

Pebble lithology and shape were determined at sites where particle size and gravel thickness were measured. Pebble counts consisted of 50–100 pebbles each, 2.5–7.6 cm (1–3 in.) in long dimension. In some cases two counts of 50 pebbles each were made from different parts of an outcrop; these were combined. Global Positioning System (GPS) locations are shown for the separate counts (table A1); data are given in tables A2–A6. Lithologic categories of Lindsey and Melick (2002) were followed with minor modification. Five pebble counts from earlier work (Lindsey and Melick, 2002) were recast because the lithologic categories differed slightly from this report; the recast counts are reported again here. Pebble roundness was classified in categories A–E (angular to well-rounded) of Pettijohn (1975, his fig. 3–24). Additional details of the method are given in Lindsey and Melick (2002) and Lindsey and others (2007).

In accord with previous investigations (Lindsey and Melick, 2002; Lindsey and others, 2007), clasts in terrace gravel are mostly subangular to rounded, with large proportions of subrounded clasts (tables A2–A6). An earlier analysis of lithology versus roundness (Lindsey and others, 2007) showed correlation between the two. A reanalysis using data collected for this report also showed correlation, but gave somewhat different details (table A7). In the new analysis, granitic rocks showed a tendency to round with transport (they did not in the 2007 analysis), whereas tuff, carbonate rocks, and quartz sandstone—all minor constituents with low counts—do not (they did in the 2007 analysis). Crystal-poor ignimbrite stands out in both analyses as a major contributor to total chi-square and shows a pronounced tendency to remain angular during transport. It is by far the most durable lithology counted. Volcanic rocks with quartz are the second most important contributor to chi-square in the current analysis (they were not in the 2007 analysis), showing a strong tendency to round during transport.

Differences between the two analyses may be due to differences in (1) drainages sampled or (2) rock identification and classification. First, the analysis of Lindsey and others (2007) relied on gravel samples taken from tributaries on both sides of the Santa Cruz River, whereas the present analysis uses a larger count based on samples from only the east side of the river. Second, the various types of volcanic-rock pebbles are notoriously difficult to identify and classify consistently, and the two pebble-count studies were made six years apart. Some lithologic categories in the chi-square tables are not comparable because a few rock types were combined differently or not at all. In particular, brown sandstone (determined to be volcanic, here combined with tuff) was kept separate from quartz sandstone and carbonate rocks. For the present analysis, combination of the last two lithologies was not necessary to meet statistical requirements, because more pebbles were counted than in the 2007 study.

Table A1. Sample locations for pebble counts of terrace gravel deposited by Madera Canyon Wash and adjacent streams (designated "south" and "north"), Montosa Canyon Wash, Cottonwood Wash, and Josephine Canyon Wash, east side of Santa Cruz River, Green Valley-Tubac area, Arizona.

[Samples locations, determined by Global Positioning System, are shown in figures 1 and 2; letters A and B refer to multiple samples at same location. Age of map units: Qh, Holocene deposits; Ql, late Pleistocene deposits; Qm, middle Pleistocene deposits; Qo, early Pleistocene deposits (see fig.1 for location of map units). Locations: UTM, universal transverse Mercator; NAD27, North American Datum 1927, zone 12]

Sample number	Tributary	Age	UTM North (NAD27)	UTM East (NAD27)	Elevation (feet)
D1A	Josephine	Qh	3492820	500638	3,503
D1B	Josephine	Qh	3492820	500638	3,503
D2A	Josephine	Ql	3493050	500865	3,535
D2B	Josephine	Ql	3492918	500533	3,534
D3A	Josephine	Qm	3492956	500253	3,548
D3B	Josephine	Qm	3492840	500093	3,470
D4	Josephine	Qo	3493818	500729	3,651
D6	Josephine	Ql	3493522	502552	3,664
D7A	Josephine	Qo	3493778	503198	3,816
D7B	Josephine	Qo	3493778	503198	3,816
D8	Josephine	Qh	3492899	501354	3,502
17	Lower Montosa	Ql	3507062	496800	3,210
19	Upper Montosa	Qo	3504568	502544	3,871
D9A	Lower Montosa	Ql	3506471	496800	3,223
D9B	Lower Montosa	Ql	3506471	496800	3,223
D11	Upper Montosa	Qm	3503776	503248	3,957
D13A	Cottonwood	Qm	3501213	503188	3,863
D13B	Cottonwood	Qm	3501213	503188	3,863
13	Madera south	Ql	3513896	500361	3,090
D20A	Madera south	Qo	3512262	503452	3,404
D20B	Madera south	Qo	3512262	503452	3,404
D23	Madera south	Ql	3511655	504789	3,476
11	Madera north	Qm	3516100	511044	3,682
12	Madera north	Qm	3523650	502773	2,900
D24A	Madera north	Qm	3515309	508777	3,675
D27	Madera north	Qm	3518148	504839	3,180

Table A2. Summary of pebble counts for terrace gravel of Madera Canyon Wash and adjacent streams (includes contributions from Florida Canyon and Chino Canyon Wash), Montosa Canyon Wash, Cottonwood Canyon Wash, and Josephine Canyon Wash, east side of Santa Cruz River, Green Valley-Tubac area, Arizona. Counts converted to percent for pie diagrams of figure 7.

Lithology	Madera Canyon Wash	Montosa Canyon Wash	Cottonwood Canyon Wash	Josephine Canyon Wash	Totals
Granitic rocks	222	73	18	119	432
Gabbro and diorite	11	32	0	7	50
Crystal-poor ignimbrite	138	13	0	33	184
Volcanic sandstone and tuff	22	54	6	39	121
Volcanic rocks with quartz	146	75	62	251	534
Volcanic rocks without quartz	48	46	14	111	219
Carbonate rocks	0	40	0	0	40
Quartz sandstone	8	13	0	1	22
Vein quartz	5	2	1	0	8
Totals	**600**	**348**	**101**	**561**	**1,610**

Table A3. Lithology versus roundness for terrace gravel of Madera Canyon Wash and adjacent streams, Green Valley-Tubac area, Arizona. *A*, North part, Florida Canyon Wash plus Madera Canyon Wash (samples 11 and 12) and Madera Canyon Wash only (samples D24A and D27). *B*, South part, Chino Canyon Wash plus Madera Canyon Wash (samples 13 and D20AB), Madera Canyon Wash only (D23), and totals for all samples, both parts.

[All data are counts. Roundness values are A, angular; B, subangular; C, subrounded; D, rounded; E, well-rounded (Pettijohn, 1975, his fig. 3–24). Ql, late Pleistocene deposits; Qm, middle Pleistocene deposits; Qo, early Pleistocene deposits. Σ, lithology totals. See table A1 and figure 1 for sample locations. "AB" refers to combined sample. Counts converted to percent for pie diagrams of figure 8]

***A.* North part, Florida Canyon Wash and middle Pleistocene Madera Canyon Wash**

Lithology	Qm sample 11						Qm sample 12						Qm sample D24A						Qm sample D27					
	Roundness						Roundness						Roundness						Roundness					
	A	B	C	D	E	Σ	A	B	C	D	E	Σ	A	B	C	D	E	Σ	A	B	C	D	E	Σ
Granitic rocks	7	15	16	3	0	41	0	1	9	3	0	13	0	0	5	3	0	8	0	1	7	3	0	11
Gabbro and diorite	0	0	1	0	0	1	0	0	0	0	0	0	0	0	0	1	0	1	0	0	0	0	0	0
Crystal-poor ignimbrite	2	23	13	0	0	38	0	26	35	5	0	66	0	2	6	0	0	8	0	2	4	0	0	6
Volcanic sandstone and tuff	0	0	2	2	0	4	0	0	1	3	0	4	0	0	3	2	0	5	0	0	3	1	1	5
Volcanics with quartz	0	0	0	0	0	0	0	0	0	0	0	0	0	1	16	5	2	24	0	2	17	8	2	29
Volcanics without quartz	0	1	9	1	0	11	0	0	9	4	0	13	0	0	4	0	0	4	0	0	0	0	0	0
Carbonate rocks	0	0	0	0	0	0	0	0	0	0	0	0	0	0	0	0	0	0	0	0	0	0	0	0
Quartz sandstone	0	0	2	2	0	4	0	0	4	0	0	4	0	0	0	0	0	0	0	0	0	0	0	0
Vein quartz	0	0	0	0	0	0	0	0	0	0	0	0	0	0	0	0	0	0	0	0	0	0	0	0
Totals	**9**	**39**	**43**	**8**	**0**	**99**	**0**	**27**	**58**	**15**	**0**	**100**	**0**	**3**	**34**	**11**	**2**	**50**	**0**	**5**	**31**	**12**	**3**	**51**

***B.* South part, Chino Canyon Wash and Madera Canyon Wash, and all samples, both parts**

Lithology	Ql sample 13						Qo sample D20AB						Ql sample D23						All samples, both parts					
	Roundness						Roundness						Roundness						Roundness					
	A	B	C	D	E	Σ	A	B	C	D	E	Σ	A	B	C	D	E	Σ	A	B	C	D	E	Σ
Granitic rocks	0	23	51	5	0	79	0	4	33	11	0	48	0	2	12	7	1	22	7	46	133	35	1	222
Gabbro and diorite	0	1	3	1	0	5	0	0	0	1	0	1	0	1	0	1	1	3	0	2	4	4	1	11
Crystal-poor ignimbrite	0	4	3	0	0	7	0	0	0	0	0	0	0	5	8	0	0	13	2	62	69	5	0	138
Volcanic sandstone and tuff	0	0	0	0	0	0	0	0	0	0	0	0	0	0	2	2	0	4	0	0	11	10	1	22
Volcanics with quartz	0	2	4	0	0	6	0	2	29	12	0	43	0	1	33	10	0	44	0	8	99	35	4	146
Volcanics without quartz	0	2	0	1	0	3	0	1	3	0	0	4	0	0	4	9	0	13	0	4	29	15	0	48
Carbonate rocks	0	0	0	0	0	0	0	0	0	0	0	0	0	0	0	0	0	0	0	0	0	0	0	0
Quartz sandstone	0	0	0	0	0	0	0	0	0	0	0	0	0	0	0	0	0	0	0	0	6	2	0	8
Vein quartz	0	0	0	0	0	0	0	3	0	0	0	3	0	2	0	0	0	2	0	5	0	0	0	5
Totals	**0**	**32**	**61**	**7**	**0**	**100**	**0**	**10**	**65**	**24**	**0**	**99**	**0**	**11**	**59**	**29**	**2**	**101**	**9**	**122**	**351**	**106**	**7**	**600**

Table A4. Lithology versus roundness for terrace gravel of Montosa Canyon Wash, Green Valley-Tubac area, Arizona.

[All data are counts. Roundness values are A, angular; B, subangular; C, subrounded; D, rounded; E, well-rounded (Pettijohn, 1975, his fig. 3–24). Ql, late Pleistocene deposits; Qm, middle Pleistocene deposits; Qo, early Pleistocene deposits. Σ, lithology totals. See table A1 and figure 1 for sample locations. "AB" refers to combined sample]

Lithology	Ql sample 17						Ql sample D9AB						Qo sample 19						Qm sample D11						All samples					
	Roundness						Roundness						Roundness						Roundness						Roundness					
	A	B	C	D	E	Σ	A	B	C	D	E	Σ	A	B	C	D	E	Σ	A	B	C	D	E	Σ	A	B	C	D	E	Σ
Granitic rocks	0	4	10	8	0	22	1	3	9	7	0	20	1	5	13	3	1	23	0	0	6	2	0	8	2	12	38	20	1	73
Gabbro and diorite	0	6	16	0	0	22	0	1	0	1	0	2	0	2	4	0	0	6	0	0	2	0	0	2	0	9	22	1	0	32
Crystal-poor ignimbrite	0	4	0	0	0	4	0	2	1	0	0	3	0	5	0	0	0	5	0	1	0	0	0	1	0	12	1	0	0	13
Volcanic sandstone and tuff	1	4	5	1	0	11	0	5	0	0	0	5	0	12	17	6	0	35	0	2	1	0	0	3	1	23	23	7	0	54
Volcanics with quartz	0	6	3	0	0	9	0	7	25	8	0	40	0	8	7	0	0	15	0	2	8	1	0	11	0	23	43	9	0	75
Volcanics without quartz	0	7	6	0	0	13	0	1	13	5	0	19	0	4	3	0	0	7	0	4	3	0	0	7	0	16	25	5	0	46
Carbonate rocks	1	7	8	0	0	16	0	2	7	2	0	11	0	2	2	0	0	4	0	6	3	0	0	9	1	17	20	2	0	40
Quartz sandstone	0	0	0	0	0	0	0	4	2	0	0	6	0	0	0	0	0	0	1	5	1	0	0	7	1	9	3	0	0	13
Vein quartz	0	2	0	0	0	2	0	0	0	0	0	0	0	0	0	0	0	0	0	0	0	0	0	0	0	2	0	0	0	2
Totals	**2**	**40**	**48**	**9**	**0**	**99**	**1**	**25**	**57**	**23**	**0**	**106**	**1**	**38**	**46**	**9**	**1**	**95**	**1**	**20**	**24**	**3**	**0**	**48**	**5**	**123**	**175**	**44**	**1**	**348**

Table A5. Lithology versus roundness for terrace gravel of Cottonwood Canyon Wash, Green Valley-Tubac area, Arizona.

[All data are counts. Roundness values are A, angular; B, subangular; C, subrounded; D, rounded; E, well-rounded (Pettijohn, 1975, his fig. 3–24). Qm, middle Pleistocene deposits. See table A1 and figure 1 for sample locations. "AB" refers to combined sample]

Lithology	Qm sample 13AB					
	Roundness					
	A	B	C	D	E	Totals
Granitic rocks	0	5	9	2	2	18
Gabbro and diorite	0	0	0	0	0	0
Crystal-poor ignimbrite	0	0	0	0	0	0
Volcanic sandstone and tuff	0	1	4	1	0	6
Volcanics with quartz	1	9	34	18	0	62
Volcanics without quartz	0	1	8	5	0	14
Carbonate rocks	0	0	0	0	0	0
Quartz sandstone	0	0	0	0	0	0
Vein quartz	0	0	1	0	0	1
Totals	**1**	**16**	**56**	**26**	**2**	**101**

Table A6. Lithology versus roundness for terrace gravel of Josephine Canyon Wash, Green Valley-Tubac area, Arizona.

[All data are counts. Roundness values are A, angular; B, subangular; C, subrounded; D, rounded; E, well-rounded (Pettijohn, 1975, his fig. 3-24). Qh, Holocene deposits; Ql, late Pleistocene deposits; Qm, middle Pleistocene deposits; Qo, early Pleistocene deposits. No vein quartz counted. Σ, lithology totals. See table A1 and figure 2 for sample locations. "AB" refers to combined sample]

Lithology	Qh sample D1AB						Qh sample D8						Ql sample D2AB						Ql sample D6					
	Roundness						Roundness						Roundness						Roundness					
	A	B	C	D	E	Σ	A	B	C	D	E	Σ	A	B	C	D	E	Σ	A	B	C	D	E	Σ
Granite	0	2	5	7	4	18	0	0	2	1	3	6	0	3	14	11	5	33	0	0	6	7	2	15
Gabbro and diorite	0	0	1	1	0	2	0	0	0	0	0	0	0	0	0	1	0	1	0	0	0	1	0	1
Crystal-poor ignimbrite	0	5	2	0	0	7	0	0	2	0	0	2	0	5	4	3	0	12	0	2	0	0	0	2
Volcanic sandstone and tuff	0	6	6	0	1	13	0	1	2	1	0	4	0	0	3	1	0	4	0	0	0	0	0	0
Volcanics with quartz	0	12	16	8	1	37	0	1	18	9	1	29	0	5	11	12	2	30	0	0	9	13	1	23
Volcanics without quartz	1	8	9	3	1	22	0	2	4	5	0	11	0	2	16	10	1	29	0	1	6	2	1	10
Carbonate rocks	0	0	0	0	0	0	0	0	0	0	0	0	0	0	0	0	0	0	0	0	0	0	0	0
Quartz sandstone	0	0	1	0	0	1	0	0	0	0	0	0	0	0	0	0	0	0	0	0	0	0	0	0
Totals	**1**	**33**	**40**	**19**	**7**	**100**	**0**	**4**	**28**	**16**	**4**	**52**	**0**	**15**	**48**	**38**	**8**	**109**	**0**	**3**	**21**	**23**	**4**	**51**

Lithology	Qm sample D3AB						Qo sample D4						Qo sample D7AB						All samples					
	Roundness						Roundness						Roundness						Roundness					
	A	B	C	D	E	Σ	A	B	C	D	E	Σ	A	B	C	D	E	Σ	A	B	C	D	E	Σ
Granitic rocks	0	1	7	8	4	20	0	0	1	2	0	3	0	1	10	9	4	24	0	7	45	45	22	119
Gabbro and diorite	0	0	1	2	0	3	0	0	0	0	0	0	0	0	0	0	0	0	0	0	2	5	0	7
Crystal-poor ignimbrite	0	4	2	0	0	6	0	0	1	0	0	1	0	2	1	0	0	3	0	18	12	3	0	33
Volcanic sandstone and tuff	0	4	3	1	0	8	0	2	5	0	0	7	0	0	3	0	0	3	0	13	22	3	1	39
Volcanics with quartz	0	1	24	17	4	46	0	4	22	3	1	30	0	1	28	23	4	56	0	24	128	85	14	251
Volcanics without quartz	0	4	12	3	0	19	0	3	5	2	0	10	0	1	9	0	0	10	1	21	61	25	3	111
Carbonate rocks	0	0	0	0	0	0	0	0	0	0	0	0	0	0	0	0	0	0	0	0	0	0	0	0
Quartz sandstone	0	0	0	0	0	0	0	0	0	0	0	0	0	0	0	0	0	0	0	0	1	0	0	1
Totals	**0**	**14**	**49**	**31**	**8**	**102**	**0**	**9**	**34**	**7**	**1**	**51**	**0**	**5**	**51**	**32**	**8**	**96**	**1**	**83**	**271**	**166**	**40**	**561**

Table A7. Chi-square analysis of pebble lithology versus roundness, combined samples of gravel deposited by Madera Canyon Wash and adjacent streams, Montosa Canyon Wash, Cottonwood Canyon Wash, and Josephine Canyon Wash.

[Roundness classes of Pettijohn (1975, his fig. 3–24): A, angular; B, subangular; C, subrounded; D, rounded; and E, well-rounded. Degrees of freedom, 14; total χ^2, 174.773; χ^2 P-value <0.0001; G^2, 176.731; G^2 P-value, <0.0001. OBS, observed frequency; EXP, expected frequency; χ^2, Pearson chi-square value; RES, adjusted residual (values of <–1.96 and >+1.96 are significant at the 0.05 level). Vein quartz was too sparse to be included in the analysis. See Lindsey and others (2007) for discussion of statistical methods]

Lithology	Roundness A+B				Roundness C				Roundness D+E				Totals
	OBS	EXP	χ^2	RES	OBS	EXP	χ^2	RES	OBS	EXP	χ^2	RES	
Granitic rocks	79	96.54	3.19	–2.37	225	229.75	0.10	–0.54	128	105.71	4.70	2.92	432
Gabbro and diorite	11	11.17	.003	–.06	28	26.59	.08	.41	11	12.24	.13	–.41	50
Crystal-poor ignimbrite	94	41.12	68.01	9.95	82	97.86	2.57	–2.49	8	45.02	30.45	–6.75	184
Volcanic sandstone and tuff	38	27.04	4.44	2.49	60	64.35	.29	–.83	23	29.61	1.48	–1.45	121
Volcanics with quartz	65	119.33	24.74	–6.91	304	284.00	1.41	2.12	165	130.67	9.02	4.23	534
Volcanics without quartz	43	48.94	.72	–1.04	123	116.47	.37	.95	53	53.59	.01	–.10	219
Carbonate rocks	18	8.94	9.19	3.48	20	21.27	.08	–.41	2	9.79	6.20	–2.90	40
Quartz sandstone	10	4.92	5.26	2.62	10	11.70	.25	–.73	2	5.38	2.13	–1.69	22
Totals	**358**	**358**	**--**	**--**	**852**	**852**	**--**	**--**	**392**	**392**	**--**	**--**	**1,602**

Appendix B. Particle Size Data

Particle size (table B1) was estimated on vertical outcrops using a field method adapted to coarse gravel and steep outcrops that are difficult to sample by sieving. The method also works with indurated gravel. A length of 50–60 in. of tape or a 55-in. walking stick was placed vertically across the outcrop, and all particles with intercepts >0.75 in. were classified into geometric classes 0.75–1.5, 1.5–3, 3–6, 6–12, and >12 in.—and counted.[1] The procedure was repeated until about 300 in. (range of 160–360 in.) was traversed. Classification of particle size only took into account the intercept of the tape or stick where it crossed a particle—no other dimension of the particle was considered. This method gives a linear measure of apparent particle size, which is proportional to area or volume in two or three dimensions. Thus particle size classified by the particle-intercept method is an estimate of relative volume, not relative weight as estimated by sieving. Counts of each size class were then multiplied by the geometric class midpoints (for example, 1.06, 2.12, 4.24, and 8.48 in. for classes 0.75–1.5 through 6–12 in.); for particle intercepts >12 in., actual measurements of intercepts were added together. Results were totaled and subtracted from the total measured length to find the frequency of < 0.75-in. particles. Finally, all class total lengths were converted into percent and plotted as cumulative frequency distributions on a metric $\log_2$ scale.

[1]Particle size classes were determined in the English system and converted to metric (SI) units for display; English particle sizes are given in tables and shown with metric sizes on frequency curves to facilitate use by the U.S. aggregate industry, which uses the English system.

Particle size determined by direct measurement in outcrops is not suitable for comparison with results from sieving, pending further work. In this report, direct measurements are compared with one another. No sieving was done to determine whether results from direct measurement can be converted to sieve equivalents.

Ideally, particle size was determined for the entire vertical thickness of each terrace deposit. In some cases, access limited measurement to only part of the deposit, but in most cases, particle size was determined for most of the vertical thickness of the terrace fill. For thick terrace fills, particle size was determined only in accessible locations that appeared to be representative of the entire thickness. The thickness of each deposit was estimated or measured where particle size was determined.

Sorting was calculated using the equation of Trask (Krumbein and Pettijohn, 1938) as the square root of P_{75}/P_{25} (largest quartile size divided by the smallest quartile size). Quartile measures (P_{25}, P_{50} (the median), and P_{75}) were determined from cumulative frequency distributions.

Terraces of major tributaries from Florida Canyon Wash to Josephine Canyon Wash on the east side of the Santa Cruz River were sampled. Terrace gravel of varying age was sampled within small, compact areas (table B2) within each piedmont drainage to enable comparison without the complicating influence of distance from the mountain front.

Table B1. Volumetric particle size data and statistics for terrace gravel of Madera Canyon Wash and adjacent streams, Montosa Canyon Wash, an unnamed tributary wash of the Santa Cruz River, Cottonwood Canyon Wash, and Josephine Canyon Wash, east side of Santa Cruz River, Green Valley-Tubac area, Arizona. Samples located in figures 1 and 2; A and B refer to multiple samples at same location, except D2A and D2B, which are from separate locations shown on figure 2. Local area refers to groups of samples located approximately the same distance from the mountain front on a given drainage.

[Stratigraphic units: Qh, Holocene deposits; Ql, late Pleistocene deposits; Qm, middle Pleistocene deposits; Qo, early Pleistocene deposits; QTs, Quaternary and Tertiary deposits. Locations: UTM, Universal Transverse Mercator; NAD27, North American Datum 1927, zone 12; ELEV, elevation. Distance from canyon mouth, where stream leaves the mountain front and enters the piedmont. Local areas: 1, Florida Canyon Wash; 2, Florida Canyon Wash near junction with middle Pleistocene Madera Canyon Wash; 3, present-day Madera Canyon Wash near junction with Chino Canyon Wash; 4, Madera Canyon Wash, upper piedmont; 5, Madera Canyon Wash, middle piedmont; 6, Montosa Canyon Wash, upper piedmont; 7, Montosa Canyon Wash, lower piedmont; 8, unnamed tributary of Santa Cruz river; 9, Cottonwood Canyon Wash; 10, Josephine Canyon Wash. Measures: m, meters; km, kilometers; ft, feet; in., inches; mm, millimeters. Parameters: Pct, percent; P_{25}, P_{50}, and P_{75} are percentiles; So, Trask sorting coefficient; --, no data]

Sample number	Local area	Unit	Thick-ness (m)	Dis-tance (km)	UTM North (NAD27)	UTM East (NAD27)	Elev (ft)	Pct <75 in.	Pct .75–1.5 in.	Pct 1.5–3 in.	Pct 3–6 in.	Pct 6–12 in.	Pct >12 in.	Pct >6 in.	Pct >3 in.	Pct >1.5 in.	Pct >0.75 in.	P_{25} (mm)	P_{50} (mm)	P_{75} (mm)	So	Log So
D1A	10	Qh	3.0	8.7	3492820	500638	3503	27.9	12.0	22.6	25.4	5.7	6.3	12.0	37.4	60.0	72.1	14	56	114	2.854	0.455
D1B	10	Qh	2.0	8.7	3492820	500638	3503	9.8	13.4	29.0	41.0	2.8	4.0	6.8	47.8	76.8	90.2	40	74	118	1.718	.235
D2A	10	Ql	2.0	8.4	3493050	500865	3535	12.0	12.3	27.5	28.9	14.5	4.8	19.2	48.2	75.7	88.0	40	74	136	1.844	.266
D2B	10	Ql	2.0	8.8	3492918	500533	3534	18.4	14.5	30.4	22.6	14.1	.0	14.1	36.7	67.1	81.6	27	60	116	2.073	.317
D3A	10	Qm	18.0	9.0	3492956	500253	3548	38.7	17.4	31.8	12.1	.0	.0	.0	12.1	43.9	61.3	10	32	60	2.449	.389
D3B	10	Qm	18.0	9.2	3492840	500093	3470	24.0	20.1	33.2	19.8	2.8	.0	2.8	22.6	55.8	76.0	20	44	74	1.924	.284
D4	10	Qo	2.0+	8.6	3493818	500729	3651	32.4	18.6	38.4	10.6	.0	.0	.0	10.6	49.0	67.6	12	37	62	2.273	.357
D6	10	Ql	8.0	6.7	3493522	502552	3664	4.3	19.0	35.3	33.3	8.0	.0	8.0	41.3	76.7	95.7	40	66	114	1.688	.227
D7A	10	Qo	20.0	6.0	3493778	503198	3816	11.0	17.0	42.7	26.7	2.7	.0	2.7	29.3	72.0	89.0	35	57	88	1.586	.200
D7B	10	Qo	20.0	6.7	3493778	503198	3816	11.3	25.3	39.3	21.3	2.7	.0	2.7	24.0	63.3	88.7	30	52	75	1.581	.199
D8	10	Qh	2.0	8.0	3492899	501354	3502	6.9	11.3	26.0	36.0	16.0	3.8	19.8	55.8	81.8	93.1	48	88	140	1.708	.232
19	6	Qo	9.0	2.7	3504568	502544	3871	40.7	11.1	21.7	15.8	8.7	1.9	10.6	26.4	48.1	59.3	7	35	82	3.423	.534
39	7	Ql	2.0	9.2	3505746	496167	3226	45.2	12.4	25.9	16.5	.0	.0	.0	16.5	42.4	54.8	6	26	63	3.240	.511
D9A	7	Ql	3.0	8.8	3506471	496800	3223	39.1	36.2	20.0	4.6	.0	.0	.0	4.6	24.7	60.9	12	24	38	1.780	.250
D9B	7	Ql	3.0	8.8	3506471	496800	3223	25.2	43.9	23.1	4.6	3.1	.0	3.1	7.7	30.8	74.8	19	30	48	1.589	.201
D11	6	Qm	5.0	3.2	3503776	503248	3957	12.4	19.1	29.0	19.8	19.8	.0	19.8	39.6	68.5	87.6	32	63	132	2.031	.308
D13A	9	Qm	3.0	2.6	3501213	503188	3863	17.3	20.9	24.1	18.8	18.8	.0	18.8	37.7	61.8	82.7	26	57	127	2.210	.344
D13B	9	Qm	3.0	2.6	3501213	503188	3863	1.3	17.0	28.3	32.5	17.0	4.0	21.0	53.5	81.7	98.7	47	84	142	1.738	.240
D14	9	Qm	2.0	3.6	3500568	502374	3752	7.1	28.6	29.0	18.4	17.0	.0	17.0	35.3	64.3	92.9	32	57	118	1.920	.283
D15	9	Qm	6.0	2.4	3501182	503362	3867	3.5	15.9	28.3	26.9	25.4	.0	25.4	52.3	80.6	96.5	45	83	154	1.850	.267
D16	7	Ql	8.0	7.6	3505432	497769	3320	18.4	25.4	33.4	15.4	2.6	4.8	7.4	22.8	56.2	81.6	24	46	74	1.756	.245
D18	7	Ql	4.0	7.3	3503195	498049	3340	8.8	38.2	33.2	14.1	5.7	.0	5.7	19.8	53.0	91.2	27	42	70	1.610	.207
D19	6	Ql	10.0	.5	3504002	504804	4141	12.6	14.1	27.1	29.4	11.8	5.0	16.8	46.2	73.3	87.4	36	70	130	1.900	.279
D20A	3	Qo	4.0	7.6	3512262	503452	3404	9.1	21.2	27.3	27.3	15.1	.0	15.1	42.4	69.7	90.9	34	66	125	1.917	.283

Table B1. Volumetric particle size data and statistics for terrace gravel of Madera Canyon Wash and adjacent streams, Montosa Canyon Wash, an unnamed tributary wash of the Santa Cruz River, Cottonwood Canyon Wash, and Josephine Canyon Wash, east side of Santa Cruz River, Green Valley-Tubac area, Arizona. Samples located in figures 1 and 2; A and B refer to multiple samples at same location, except D2A and D2B, which are from separate locations shown on figure 2. Local area refers to groups of samples located approximately the same distance from the mountain front on a given drainage.—Continued

[Stratigraphic units: Qh, Holocene deposits; Ql, late Pleistocene deposits; Qm, middle Pleistocene deposits; Qo, early Pleistocene deposits; QTs, Quaternary and Tertiary deposits. Locations: UTM, Universal Transverse Mercator; NAD27, North American Datum 1927, zone 12; ELEV, elevation. Distance from canyon mouth, where stream leaves the mountain front and enters the piedmont. Local areas: 1, Florida Canyon Wash; 2, Florida Canyon Wash near junction with middle Pleistocene Madera Canyon Wash; 3, present-day Madera Canyon Wash near junction with Chino Canyon Wash; 4, Madera Canyon Wash, upper piedmont; 5, Madera Canyon Wash, middle piedmont; 6, Montosa Canyon Wash, upper piedmont; 7, Montosa Canyon Wash, lower piedmont; 8, unnamed tributary of Santa Cruz river; 9, Cottonwood Canyon Wash; 10, Josephine Canyon Wash. Measures: m, meters; km, kilometers; ft, feet; in., inches; mm, millimeters. Parameters: Pct, percent; P_{25}, P_{50}, and P_{75} are percentiles; So, Trask sorting coefficient; --, no data]

Sample number	Local area	Unit	Thick-ness (m)	Dis-tance (km)	UTM North (NAD27)	UTM East (NAD27)	Elev (ft)	Pct <75 in.	Pct .75–1.5 in.	Pct 1.5–3 in.	Pct 3–6 in.	Pct 6–12 in.	Pct >12 in.	Pct >6 in.	Pct >3 in.	Pct >1.5 in.	Pct >0.75 in.	P_{25} (mm)	P_{50} (mm)	P_{75} (mm)	So	Log So
D20B	3	Qo	4.0	7.6	3512262	503452	3404	17.5	11.4	28.8	33.3	9.1	.0	9.1	42.4	71.2	82.5	32	66	116	1.904	.280
D22	3	Ql	5.0	6.6	3511573	504458	3430	0.6	19.4	34.7	22.4	18.8	4.0	22.9	45.3	80.0	99.4	44	70	145	1.815	0.259
D23	3	Ql	7.0	6.3	3511655	504789	3476	.2	18.9	30.1	29.3	21.6	.0	21.6	50.9	80.9	99.8	46	78	144	1.769	.248
D24A	4	Qm	6.0	4.2	3515309	508777	3675	9.6	16.8	17.6	33.6	22.4	.0	22.4	56.0	73.6	90.4	36	90	146	2.014	.304
D24BL	4	QTs	--	--	3515277	508864	3647	19.0	14.9	25.7	32.0	8.3	.0	8.3	40.3	66.0	81.0	26	60	113	2.085	.319
D24BU	4	Qh	1.0	4.2	3515277	508864	3647	6.9	12.9	24.7	31.7	14.1	9.7	23.8	55.5	80.2	93.1	47	90	150	1.786	.252
D24C	4	Qm	8.0	4.2	3515209	508895	3680	17.2	17.0	26.8	27.5	11.6	.0	11.6	39.1	65.8	82.8	28	60	116	2.035	.309
D25A	2	Qm	5.0	4.4	3515870	510918	3682	4.2	29.4	28.9	22.4	11.8	3.3	15.1	37.5	66.3	95.8	33	59	120	1.907	.280
D25B	2	Qm	4.0	4.4	3515935	510866	3682	19.8	12.0	20.5	22.6	19.8	5.3	25.1	47.7	68.2	80.2	26	72	152	2.418	.383
D25C	2	Qm	--	4.4	3516000	510814	3681	22.7	26.9	22.1	14.1	14.1	.0	14.1	28.3	50.4	77.3	21	38	93	2.104	.323
D26	1	Ql	1.0	10.0	3520299	506257	3194	4.8	20.5	29.7	28.7	16.4	.0	16.4	45.1	74.8	95.2	38	70	130	1.850	.267
D27	5	Qm	4.0	9.0	3518148	504839	3180	19.3	33.0	26.5	18.8	2.4	.0	2.4	21.2	47.7	80.7	23	36	70	1.745	.242
D28	5	Qm	3.0	9.0	3517390	504114	3172	9.0	36.2	31.8	19.4	3.5	.0	3.5	23.0	54.8	91.0	27	44	74	1.656	.219
D29	8	Qm	2.0	6.8	3501535	498673	3430	15.9	38.2	23.3	19.8	2.8	.0	2.8	22.6	45.9	84.1	24	36	72	1.732	.239

Table B2. Classification of particle size samples by local area and stratigraphic unit, terrace gravel of Madera Canyon Wash and adjacent streams, Montosa Canyon Wash, unnamed tributary wash, Cottonwood Canyon Wash, and Josephine Canyon Wash, east side of Santa Cruz River, Green Valley-Tubac area, Arizona.

[Stratigraphic units: Qh, Holocene deposits; Ql, late Pleistocene deposits; Qm, middle Pleistocene deposits; Qo, early Pleistocene deposits; QTs, Quaternary and Tertiary deposits]

Local area	Stratigraphic unit					Totals
	Qh	Ql	Qm	Qo	QTs	
1, Florida Canyon Wash	0	1	0	0	0	1
2, Madera-Florida Canyon junction	0	0	3	0	0	3
3, Madera Canyon Wash, present course	0	2	0	2	0	4
4, Madera Canyon Wash, upper piedmont	1	0	2	0	1	4
5, Madera Canyon Wash, lower piedmont	0	0	2	0	0	2
6, Montosa Canyon Wash, upper piedmont	0	1	1	1	0	3
7, Montosa Canyon Wash, lower piedmont	0	5	0	0	0	5
8, Unnamed tributary wash	0	0	1	0	0	1
9, Cottonwood Canyon Wash	0	0	4	0	0	4
10, Josephine Canyon Wash	3	3	2	3	0	11
Totals	**4**	**12**	**15**	**6**	**1**	**38**

Publishing support provided by:
Denver Publishing Service Center

For more information concerning this publication, contact:
Team Chief Scientist, USGS Central Mineral Resources
Box 25046, Mail Stop 973
Denver, CO 80225
(303) 236-1562
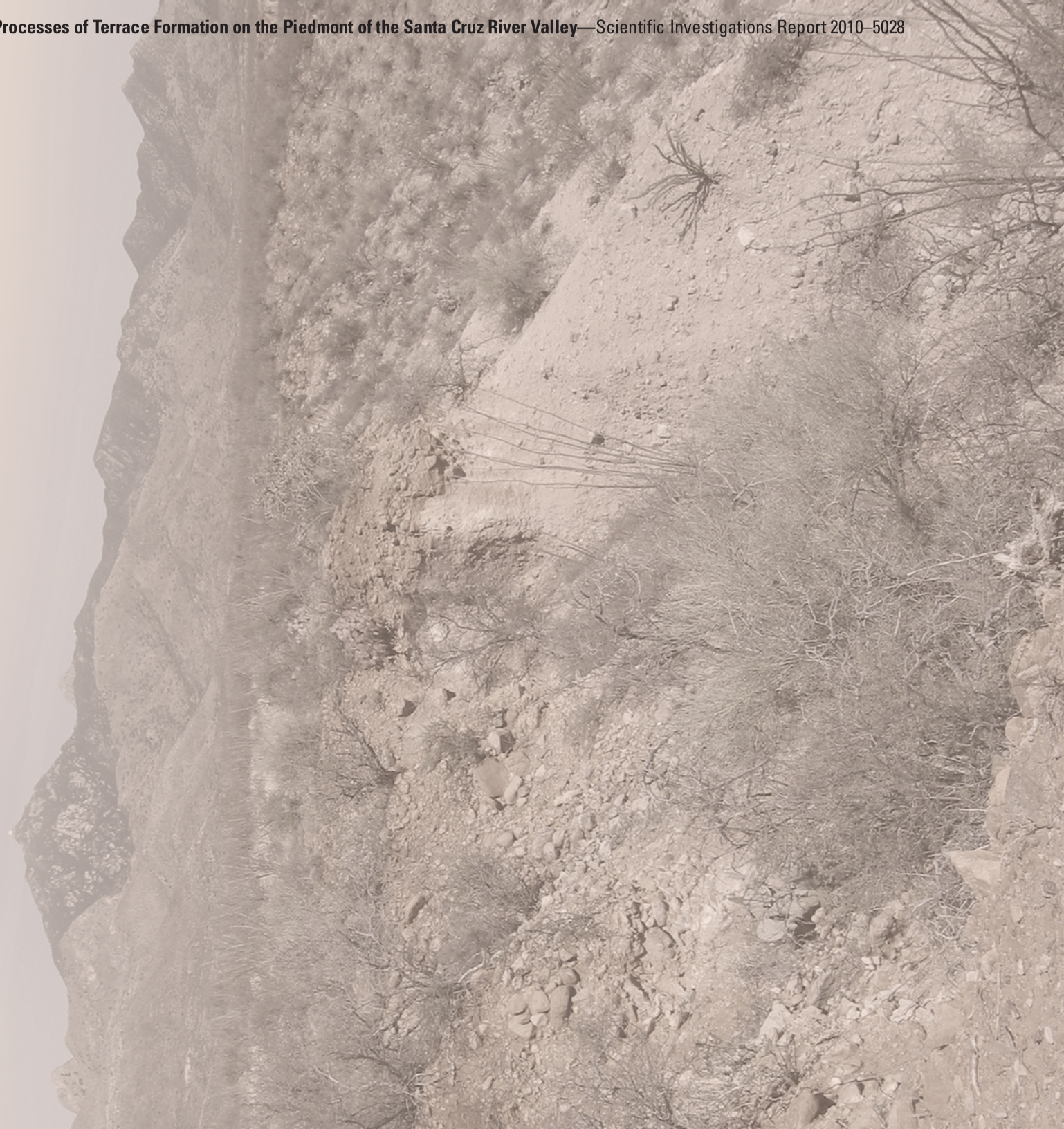
Or visit the Central Mineral Resources Team Web site at:
http://minerals.cr.usgs.gov/